Development of a Novel Dynamic Spinal Implant

&

Finite Element Modeling of L3-L4 Segment

by

Enis AKGÜN

A Thesis Submitted to the

Graduate School of Engineering

in Partial Fulfillment of the Requirements for

the Degree of

Master of Science

in

Mechanical Engineering

Koc University

August 2010

Koç University

Graduate School of Sciences and Engineering

This is to certify that I have examined this copy of a master's thesis by

Enis AKGÜN

and have found that it is complete and satisfactory in all respects,

and that any and all revisions required by the final

examining committee have been made.

Committee Members:

İsmail Lazoğlu, Ph.D. (Advisor)

Halil Kavaklı, Ph.D.

Şevket Ruacan, Ph.D.

Date: 18.08.2010

ABSTRACT

Low back pain due to disc degeneration is a worldwide major health problem at any age, but especially at an elderly age. In the treatment of low back pain, dynamic stabilization may provide a more physiologic alternative to fusion. In this study, initial model of dynamic implant was developed that limit abnormal motion at the segment while preserves the motion within normal physiological limits. The effects of design parameters to strength and flexibility of the implant were investigated. Initial design was improved to final design that builds balance between flexibility and strength.

Finite element model of an intact L3-L4 lumbar segment was developed. Load sharing characteristic of implant and effect of implant to segmental range of motion are two main criteria in evaluation of the newly developed implant. Finite element analysis were performed to investigate effects of newly developed implant to the segmental range of motion and load sharing characteristics in lateral bending, flexion, extension, and axial rotation. In this study, intact L3-L4 model and four types of screw-implant systems were investigated. These systems were rigid screw-rigid rod system, rigid screw-dynamic implant system, polyaxial screw-rigid rod system, and polyaxial screw dynamic implant system.

The polyaxial screw-dynamic implant system exhibits the best results for range of motion and load sharing characteristics within four stabilization systems. The reduction of motion for the polyaxial screw-dynamic implant system in all loading is minimum within four stabilization systems. This stabilization system shares load with the intervertebral disc and the facet joints. The rigid screw-rigid implant system greatly reduces the motion in all loading. Performances of other two stabilization systems in range of motion and load sharing are lying between the polyaxial screw-dynamic implant system and the rigid screw-rigid implant system.

ÖZET

Kronik bel ağrısı tüm dünyada başta yaşlıları olmak üzere her yaş grubundaki insanları ilgilendiren önemli bir sağlık sorunudur. Kronik bel ağrısı tedavisinde dinamik sabitleme yöntemi füzyon cerrahisine alternatif olarak kullanılan daha fizyolojik bir tedavi yöntemidir. Bu çalışmada, hasta omurga segmentinde anormal hareketliliği kısıtlayan ve segment hareketliliğini normal fizyolojik sınırlar içinde kalmasını sağlayan dinamik sabitleme implantı geliştirildi. Tasarım parametrelerinin implant dayanıklığına ve esnekliğine etkileri incelenmiştir. Bu incelemeden sonra ilk implant tasarımı dayanıklılık ve esneklik arasında denge kuracak şekilde geliştirildi.

Sağlıklı L3-L4 omurga segmentinin sonlu elemanlar modeli oluşturuldu. Yeni geliştirilen implantın değerlendirilmesinde iki temel kriter; yük paylaşımı özelliği ve implantın hareket kabiliyetidir. Yeni geliştirilen implantın lateral eğilme, fleksiyon, ekstansiyon ve eksenel dönme hareketleri için uygulanan segmentin hareketliliğine etkileri ve uygulanan segmentle implant arasındaki yük paylaşımı sonlu elemanlar yöntemi kullanılarak incelendi. Bu çalışmada, sağlıklı L3-L4 omurga segmenti ve dört farklı vida implant sistemi incelendi. Bu vida implant sislemleri şunlardır: Rijit vida rijit implant sistemi, rijit vida dinamik implant sistemi, poliaksiyal vida rijit implant ve poliaksiyal vida dinamik implant sistemi

Poliaksiyal vida dinamik implant sistemi yük paylaşımı özelliği ve implantın hareket kabiliyeti bakımından en iyi sonuçları göstermiştir. Poliaksiyal vida dinamik implant sistemi, uygulanan segmentte tüm sistemler arasında en az hareketlilik kaybına neden olmuştur. Bunun yanında, bu sistem disk ve fasetlere de yük aktarmıştır. Rijit vida rijit implant sistemi ise tüm hareket yönlerinde uygulanan segmentte büyük miktarda hareketlilik kaybına neden olmuştur. Diğer iki sabitleme sisteminin yük paylaşımı özelliği ve implantın hareket kabiliyeti bakımından performansları rijit vida rijit implant sistemi ile poliaksiyal vida dinamik implant sistemleri arasındadır.

ACKNOWLEDGEMENTS

I would like to express my deepest gratitude to my supervisor Assoc. Prof. İsmail Lazoğlu for his guidance, advice, criticism, encouragement and insight throughout the study.

The members of my dissertation committee, Prof. Dr. Şevket Ruacan and Asst. Prof. Halil Kavaklı, let me their experience, advice, and comments, for which I am extremely grateful.

I am also grateful for the helps of İskender Yılgör and Emel Yılgör.

I am very grateful to the members of American Hospital especially Ali Fahir Özer, Tuncay Kaner, Evren Keleş, Mehdi Sasani, and Tunç Öktenoğlu for their guidance and helpful suggestions. I would like to thank American Hospital for their financial support.

The author was supported by The Scientific and Technological Research Council of Turkey (TÜBİTAK) with National Scholarship Program for M.Sc. Students (Program no: BİDEB 2228).

I would like to take this opportunity to thank the staff at the MARC laboratory especially Coskun İslam, Daulet Izbassarov, Hasan Sinan Bank, Muzaffer Bütün, Fatih Şenbabaoğlu, and Yaman Boz for their constant support and conversations during my graduate studies at Koç University .

I would like to thank Yasemin who makes my life more beautiful.

I am deeply in debt to my mother, Hatice, my sister, Hale and my brother Gürkan for their encouragement and faith in me.

TABLE OF CONTENTS

LIST OF FIGURES

LIST OF TABLES

NOMENCLATURE

FSU	Functional Spine Unit
ALL	Anterior Longitudinal Ligament
PLL	Posterior Longitudinal Ligament
LF	Ligamentum Flavum
CL	Facet Capsular Ligaments
ISL	Interspinous Ligament
SSL	Supraspinous Ligament
ITL	Intertransverse ligament
FEM	Finite Element Modeling
FEA	Finite Element Analysis
IVD	Intervertebral Disc

Chapter 1 : Introduction

1.1. Overview

This chapter discusses the importance of studying the lumbar spine. Low back pain and the evolution of surgical techniques for its treatment will be discussed in the chapter. The advantages of non-fusion treatment options over the conventional fusion will be identified. This will be followed by a brief description of finite element analysis, and importance of finite element analysis in spine biomechanics. Finally, objective of the study and thesis outline will be addressed.

1.2. Significance of Low Back Pain

Low back pain is a debilitating disease that may strike people of any age. Based on past trends, it is predicted that in the United States, eight out of ten people will have lower back problems at some point of time in their life. In the United States, back pain is the second most common reason cited for visiting a physician and the most common reason for limited activity in people younger than age 45. It is also the fifth most common reason for being admitted to a hospital and the third most common cause for having surgical procedure [1-3]. Chronic back pain is the number one reason for healthcare expenditures in the United States [4]. In 2005, $86 billion was spent on back pain, up from $52 billion in 1997 [5]. Hence there is a need to understand the importance and development of low back pain treatment techniques.

1.3. The Cause of Low Back Pain and Treatments

The cause of low back pain is patient specific and highly variable and may be due to several different disease states. However, disc degeneration disease is the most common disabling spinal disease. Intervertebral disc is an important part for load carrying as well as providing segmental stability. Acute and continuous loading

may result in disc degeneration. Degenerated disc loses the height and hydration which might compress the existing nerve root and that may result in pain. The annular fibers undergo some fatigue failure and decomposition begins, resulting in immunological and inflammatory responses [6].

Disc height reduction is followed by annulus bulging which eventually causes narrowing of the spinal canal. This is also called spinal stenosis. Spinal stenosis has potential to cause back pain. Patients with spinal stenosis often feel pain decreases when the spine is in a slightly flexed position, relieving pressure within the lumbar canal [6]. Spinal stenosis is often treated by decompression laminectomy or facetectomy surgery [7]. In a laminectomy procedure, the spinous process and lamina are removed at the level of stenosis along with associated ligaments [6, 8]. The facet joints may also be partially or completely removed in a facetectomy [9].

Facet joints may also be the cause of low back pain. The facet joints are innervated by the medial branch of the posterior primary ramus of the exiting spinal nerve [10-11]. The joint capsule is also fully innervated and may lead to further pain [10]. It has been suggested that a cortisone injection to the facet reduces pain in some patients and can be used as a diagnostic tool to determine other spinal diseases [6, 10-11]. Facet hypertrophy may cause nerve root irritation due to projection of the facet into the spinal canal, thereby pinching nerves [6]. Controversy exists whether severe facet tropism (asymmetry of the bilateral facet joints) causes pain. Several authors have claimed a relationship between tropism and disc degeneration so that pain would be felt, while others find no relationship or pain indication [12-14].

In the initial stages of the low back pain (LBP), the doctors choose conservative treatments like traction, exercise, heat therapy or mobilization of the joint. Surgery is recommended for the patient to whom the back pain limits their daily activities. Treatment options may vary from conservative treatment to fusion [15-16].

Fusion is a traditional technique that has been used for stabilization till today. Fusion involves immobilizing a motion segment using bone grafts or mechanical devices such as cages as a replacement for the natural intervertebral disc. However, fusion is only 50% to 70% successful in clinical trials [4]. While fusion relieves back

pain initially, pain is likely to return due to facet hypertrophy, facet arthropathy, spinal stenosis, osteophyte formation, and posterior muscular debilitation, as well as disc degeneration at adjacent levels to the fusion site [4]. Motion at the index level is completely restricted with the fusion device which puts additional burden on the levels above and below the index level. This causes increase in adjacent level degeneration over time [17-18]. A long term follow up on lumbar fusion patients by Lehmann et al. showed that degeneration at the adjacent level was noticed in 45% of their patients. Thus, young patients are likely to have additional spine surgery due to "fusion disease" [17-18].Therefore, non-fusion techniques are currently being investigated and often used for treatment options.

Various non fusion technologies have been evolved to replace the conventional fusion techniques and are mainly intended to restore inter segmental motion. Mainly they are intended to provide physiological motion at the treated level and the adjacent level. New techniques include artificial discs, nucleus replacement techniques, interspinous spacers, and dynamic stabilization devices. Dynamic stabilization devices have many advantages over other techniques: surgical procedure is very easy, minimally invasive and better load sharing between the spinal elements. They aim at preserving the motion at the implanted level thereby minimizing the adjacent level degeneration [19].

Worldwide spinal market revenues were less than $100 million in 1990, grew to $3.5 billion by 2004, and reached more than $6 billion in 2007. It is estimated that by 2010 the US spine industry will earn more than $10 billion in revenue, with non-fusion products comprising more than 90% of the revenues [20]. Growth of the segment has indeed been impressive. As the huge young population ages, there is a growing need to develop innovative new types of spinal implants for the benefit of society. Besides, technology development in the spine field is approximately 15 years behind that of other orthopedic areas such as hip and total knee related implants [21].

1.4. Importance of Finite Element Modeling in Spine Biomechanics

In recent years, researchers have begun to apply computer modeling to the field of biomedical engineering as finite element modeling (FEM), allowing the performance of studies under pseudo *in-vivo* conditions. By using FEA, newly created implants can be adapted to better match the mechanical characteristics of actual tissue before it is prototyped. More recently, FEA models have shown to successfully model the human spine, providing insights into spine biomechanics [22-23].

Finite element analysis allows researchers to repeat experiments, change parameters, and thus analyze the effect and influence of a single entity within a complex assembly, offering valuable insights into a wide range of situations. Also, it is possible to obtain information that is not accessible through experimentation, such as the stress distribution through the intervertebral disc. Finite element analysis helps to understand how newly created implant affects the kinematics of spine such as segmental motion, adjacent level effects, load sharing. As well as for intact spine, finite element modeling can be a valuable tool in simulating biomechanical features of spine in its injured and surgically altered states.

1.5. Objective of the Study

The overall objectives of this research are to develop a novel dynamic spinal implant that stabilizes the spine segment while preserves the motion within normal physiological limits and to investigate effects of newly developed implant to the kinematics of spine by finite element modeling of L3-L4 intact spine segment. The specific goals are the following.

- Development of an initial implant model that limits abnormal motion at the segment while preserves the motion within normal physiological limits.
- Investigating the effects of design parameters to strength and flexibility of the implant.
- Improving initial design to build the balance between flexibility and strength.

- Development of anatomically accurate lumbar spine 3-D model based on Computed Tomography (CT) scans of a healthy individual.
- Development finite element model of an intact lumbar segment L3-L4.
- Performing finite element analysis of L3-L4 model to represent lateral bending, flexion, extension, axial rotation under normal physiologic loading conditions.
- Validation of the L3-L4 model through comparison with other models in literature.
- Investigation of effects of newly developed implant to the segmental range of motion (ROM) and load sharing characteristics between the implant and spine segment.

1.6. Thesis Outline

Chapter 2 covers anatomical background of the spine such as geometry, mechanical characteristics, and functions. In addition, Chapter 2 describes disorders causing low back pain, treatment options, and designs of various dynamic stabilization systems and their history.

Chapter 3 describes development procedure of a novel dynamic spinal implant. Initial implant design is rigid rod with a helical cut and a hole at the center. Chapter 3 explains improvement procedure of initial design to built balance between strength and flexibility.

Chapter 4 discusses the literature review of past spine models. A detailed summary of results and studies regarding spine biomechanics are explained. In addition, Chapter 4 describes steps of building the finite element models, including the creation of the ligament and annulus fibers. Chapter 4 explains simulation procedure of L3-L4 model for lateral bending, flexion, extension, and axial rotation

Chapter 5 presents the biomechanical data for the developed dynamic spinal implant obtained from finite element analysis of L3-L4 model.

Chapter 6 covers a summary of the results and their significance. Recommendations are made for future improvements to the modeling and simulations.

Chapter 2 : Spine and Dynamic Stabilization

2.1. Overview

This chapter covers anatomical background of the spine such as geometry, mechanical characteristics, and functions. In addition, Chapter 2 describes disorders causing low back pain, treatment options, and designs of various non fusion systems and their history.

2.2. Anatomy of Spine

First of all, some terminology of anatomy should be defined before focusing on the spine anatomy.

Human body is divided into several standardized planes and directions so that different regions of the body can be referred to quickly and without confusion. The directions and planes are described in the Figure 2.1. Frontal/Coronal plane divides human body into front and back. Sagittal plane divides into right and left parts whereas transverse plane divides human body into top and bottom parts. Lastly, median plane is a special case of the sagittal plane that runs through the midpoint of a structure. Posterior is the back, and anterior is the front. Medial means toward the midline of the body. Lateral means away from the midline of the body. Superior is toward the head end of the body. Inferior means away from the head [24].

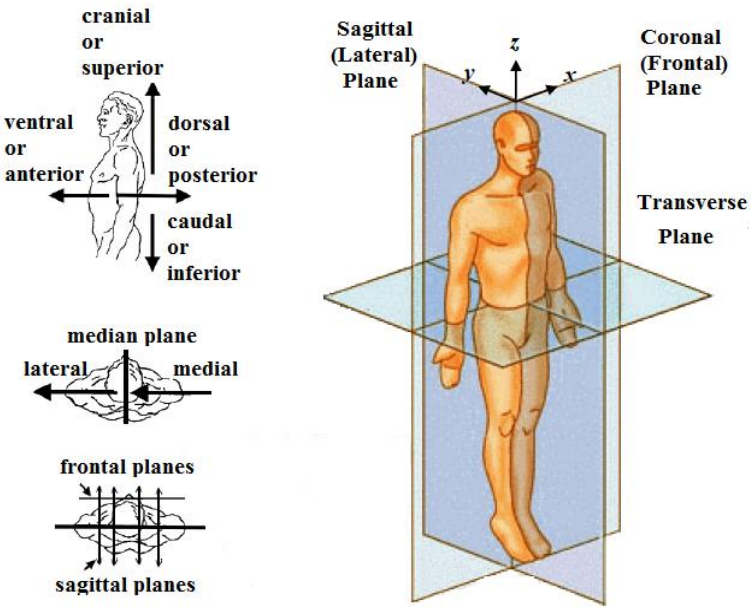

Figure 2.1: Anatomical planes and directions **[**24]

The spine is composed of 33 vertebrae distributed into five sections as shown in the Figure 2.2. Their names are the cervical spine, the thoracic spine, the lumbar spine, the sacral spine, and the coccygeal spine. This thesis focuses on the lumbar part of the spine. As shown in the Figure 2.2, the vertebral column is not straight, but consists of four curves. Two of them are convex anteriorly in the cervical and lumbar regions while the others are convex posteriorly in the thoracic and sacral regions. These curves provide flexibility and additional shock absorbing capacity to the spine [24].

The lumbar spine consists of 5 vertebral bodies and has a lot more motion than thoracic spine. These vertebral bodies are the largest of the spine and they carry the majority of the body's weight and related biomechanical stress. The pedicles are longer and wider than those in the thoracic spine. The spinous processes are horizontal and more squared in shape. The facet joints of the lumbar spine are aligned such that they allow more flexion/extension than rotation [24].

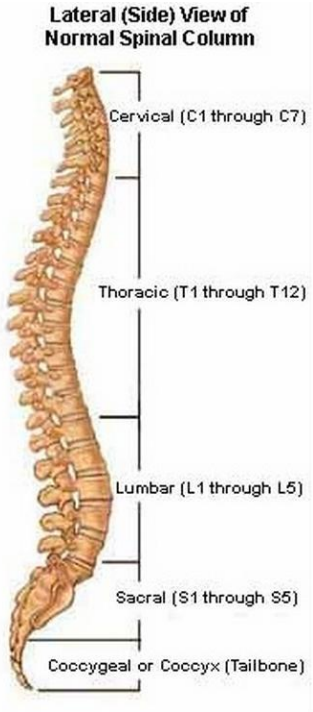

Figure 2.2: The parts of spinal column **[**25]

Spine has three major functions. First, it transfers the weight and the resultant bending moments of the head, trunk, and any weight being lifted to the pelvis. Second, it allows sufficient physiologic motions between head, trunk, and pelvis. Finally, it protects the delicate spinal cord from potentially damaging forces and motions [26].

2.3. Functional Spinal Unit (FSU)

Functional spinal unit consists of a pair of adjacent vertebrae, the intervertebral disc, facet joints, and ligaments. FSU and muscles controls the motion of spine. Figure 2.3 describe five category of spine motion: axial compression, flexion, extension, lateral bending, and axial rotation.

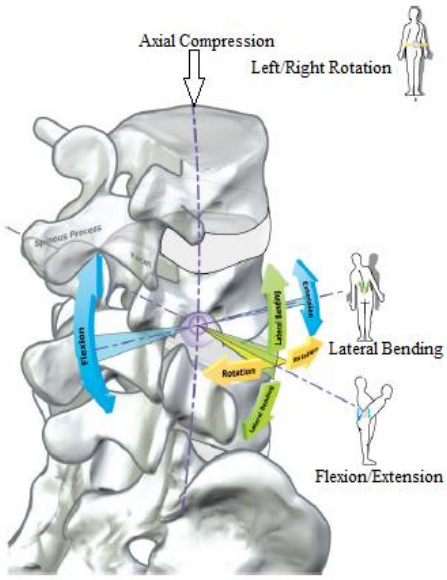

Figure 2.3: The categories of spine motion [25]

The range of motion (ROM) in each FSU is different for each region of the spine. The range of motion is determined by several structures, including ligaments, the disc, the facets, and the spinous processes. Ligament tension limits displacements between two separating elements. Facets and spinous processes limit range of motion via contacting surfaces. Strains in the intervertebral disc restrain motion between the endplates. Typical ranges of motion (ROM) for the lumbar spine are also listed in Table 2.1 [27].

Table 2.1: The physiology of range of motion of the spine [27]

FSU LEVEL	Flexion + Extension		Lateral Bending		Axial Rotation	
	Limits (°)	Typical(°)	Limits (°)	Typical(°)	Limits (°)	Typical(°)
L1-L2	5° - 16°	12°	3° - 8°	6°	1° - 3°	2°
L2-L3	8° - 18°	14°	3° - 10°	6°	1° - 3°	2°
L3-L4	6° - 17°	15°	4° - 12°	8°	1° - 3°	2°
L4-L5	9° - 21°	16°	3° - 9°	6°	1° - 3°	2°
L5-S1	10° - 24°	17°	2° - 6°	3°	0° - 2°	1°

2.3.1. Vertebrae

The vertebra consists of two distinct regions, anterior vertebral body and posterior bony element, as shown in Figure 2.4. Posterior elements are the pedicle, the lamina, and the processes. The posterior elements of the vertebra are the attachment points for many of the vertebral muscles and also serve to protect the spinal cord. Connection between the posterior elements and the vertebral body is achieved through two pedicles [28]. The cross sectional area of anterior vertebral body increases as it descends the spinal column to support the more compressive forces.

The anterior vertebral body is comprised of two different types of bone: cortical and cancellous, as shown in figure 2.5. The cortical bone is a thin and high density shell which covers all cancellous bone. Silva et al. used computed tomography (CT) to measure the thickness of cortical bone [29]. The average thickness of cortical bone is approximately 0.35mm. While the cortical bone is stiffer than the trabecular bone, it is vulnerable to fracture when the tensile strain exceeds 2%. However, trabecular bone structure can withstand greater strains [30]. The cancellous bone is structured of an interconnected network of rod and plate line trabeculae. The mechanical behavior is anisotropic, however in this thesis the cancellous bone is modeled as isotropic elastic material. The superior and inferior surfaces of the cortical bone are called as the endplates. The endplates are the interfaces between the vertebrae and the disc. they consists of hyaline cartilage in the young and become bony through aging [6]. The vertebra is modeled as five parts in this study: inferior and superior endplate, posterior vertebrae, cortical and cancellous bone.

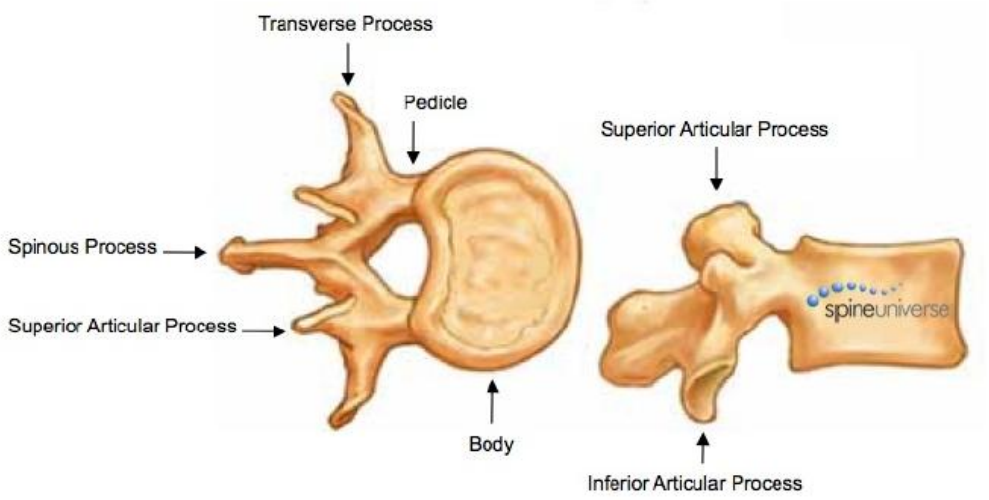

Figure 2.4: Anatomy of a vertebra body [25]

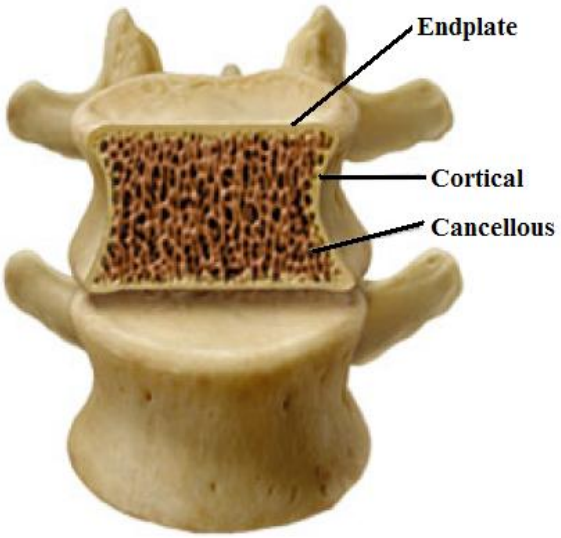

Figure 2.5: The bony structures of vertebra [25]

2.3.2. Intervertebral Disc (IVD)

The intervertebral disc is between two adjacent vertebrae, and serves as a shock absorber. It is arguably the most widely studied anatomic structure for the entire spine due to its significant role in spinal motion and injury [6]. IVD is comprised of two distinct components: the central nucleus pulposus and the periphery annulus fibrosus. (Figure 2.6)

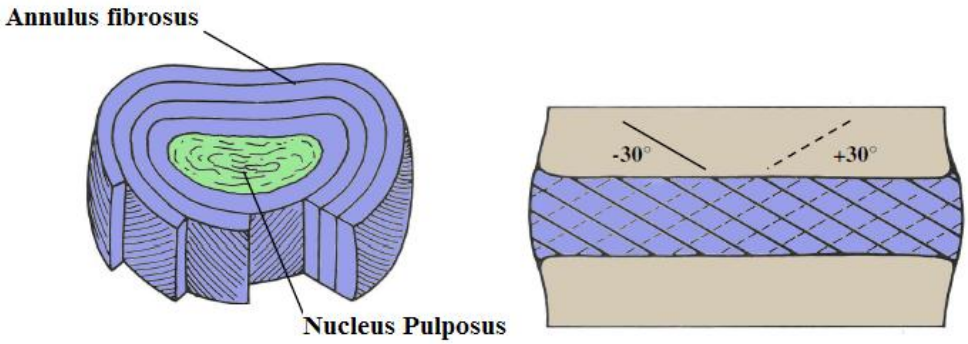

Figure 2.6: Concentric layers of the annulus fibrosus [6]

The nucleus pulposus is in the center surrounded by the annulus fibrosus. It makes up approximately 30-60 % of the cross sectional area of the non-degenerative IVD. Incompressible property of the nucleus pulposus provide to redistribute the stress through the disc bulging. Incompressible property comes from high water content which is around 70-90% volume in the nucleus [6]. In the recent studies, the nucleus modeled as fluid like material with Poisson's ratio approximately 0,5 and small elastic modulus.

The annulus fibrosus has a composite structure consisting of a series of parallel collagen fibers in a ground substance. The annulus fibrosus has different concentric layers from the innermost to the outermost boundary of the disc. The direction of fibers in each layers typically alternately from +/- 30°, as shown in Figure 2.6. The annulus fiber content is approximately 19% of annulus fibrosus in volume [6]. The strength of fibers decreases from outermost layer to innermost layer. The ground substance is a rubber like material with a small elastic modulus.

The physiological behavior of the intervertebral disc is a result of the interaction of the annulus fibrosus and the nucleus pulposus. When a compressive load is applied to a disc, hydrostatic pressure increases in the nucleus. This pressure causes radial forces to act on the layers of annulus fibrosus, resulting in the disc bulging outwards, as shown in Figure 2.7. The bulging of the annulus fibrosus puts the annular fibers in tension, which resists further deformation of the annulus and supports the hydrostatic pressure within the nucleus [6].

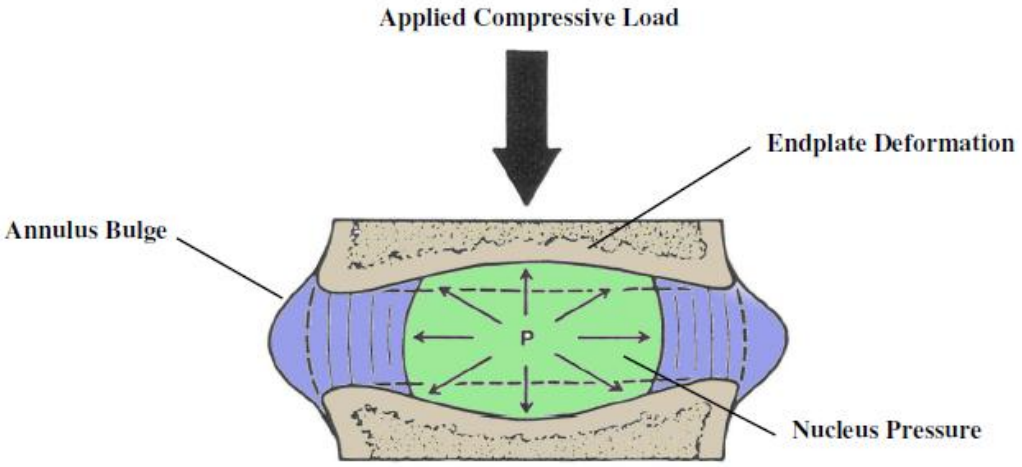

Figure 2.7: Pressure in the nucleus forcing the annulus to bulge outward [6]

In bending, the nucleus acts as a pivot for the vertebrae to rotate around. In flexion, the posterior section of the disc will be subject to tension loading that causes the annulus to contract toward the centre of the disc. The anterior section of the disc will bulge outward from the disc due to compressive loading. This will cause the nucleus to shift slightly to the posterior of the disc, as shown in Figure 2.8. The opposite is true for extension. The nucleus is not under significant hydrostatic pressure in bending.

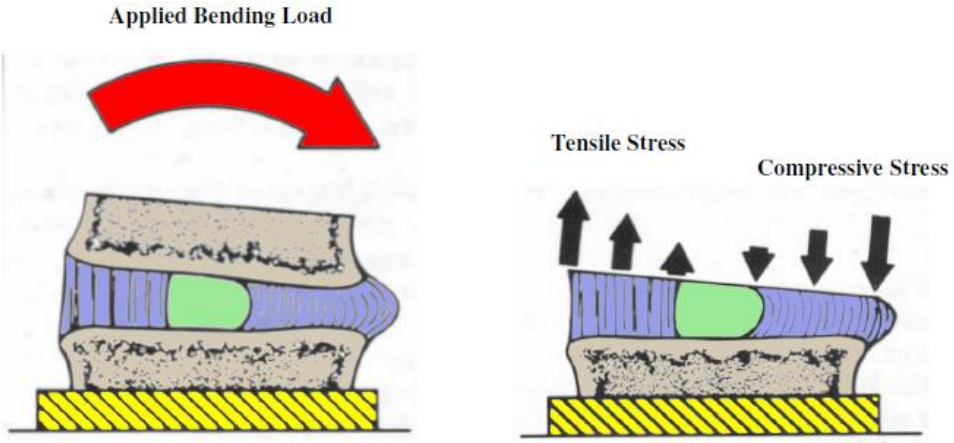

Figure 2.8: Bulging and stress distribution of the annulus from disc segment bending [6]

2.3.3. The Facet Joints

Each vertebra has two pairs of facet joints. One pair facing upwards is the superior articular facet, and the other pair facing downwards is the inferior articulating facet. The facet joints are important for two main reasons. They are a direct source for pain, and they are a principal structure for spine stability. They carry a part of the compressive loads (up to 33%) along with the vertebral body [6]. These joints are formed between articular surfaces of adjacent vertebrae, and are a complex structure of fluid, hard, and soft tissue. Facet joints limit primarily axial rotations and extension in the lumbar spine.

2.3.4. The Spinal Ligaments

Spinal ligaments are uniaxial structures comprised of fibrous bands or sheets of connective tissue that are most effective in carrying tensile loads along the direction that the fibers run. The spinal ligaments provide resistance to tensile forces, but buckle under compression [6]. A Functional Spinal Unit (FSU) includes the following 7 ligaments: the anterior longitudinal ligament, the posterior longitudinal ligament, the ligamentum flavum, the facet capsular ligaments, the interspinous ligament, the supraspinous ligament, and the intertransverse ligament, as shown in Figure 2.9.

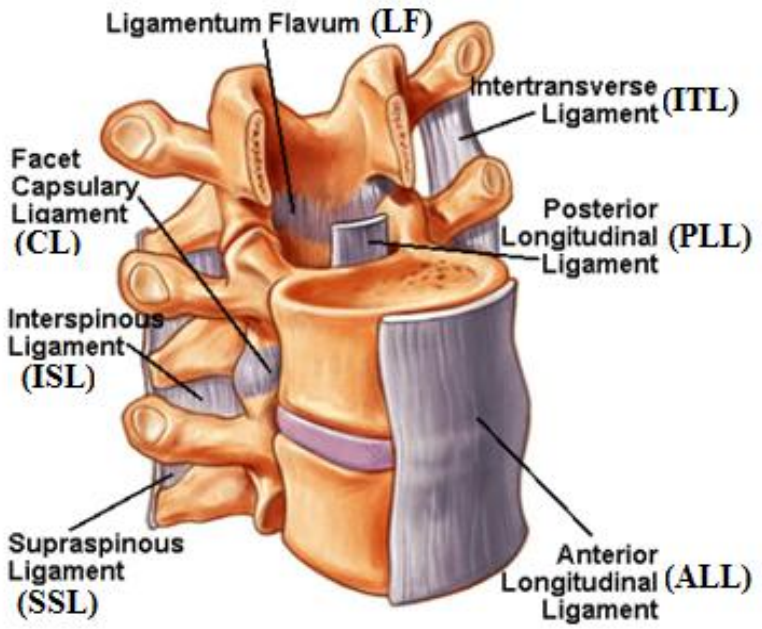

Figure 2.9: The spinal ligaments [25]

The anterior longitudinal ligament (ALL) traverses the anterior surface of the entire spine. ALL primarily restricts motion in extension. The posterior longitudinal ligament (PLL) traverses the posterior surface of the entire spine. The ligamentum flavum (LF) is the most elastic ligament, helps protect the spinal cord, and connects to adjacent lamina. The facet capsular ligaments (CL) surround the facet joint. CL is oriented perpendicular to the facet surface helping to provide stability in flexion. The interspinous ligament (ISL) is attached to adjacent spinous processes in the sagittal plane and helps to resist flexion. The supraspinous ligament (SSL) runs along the posterior edge of the spinous process. SSL helps stability in flexion. The intertransverse ligament (ITL) attaches to neighboring transverse processes and restricts motion in bending and axial rotation [6].

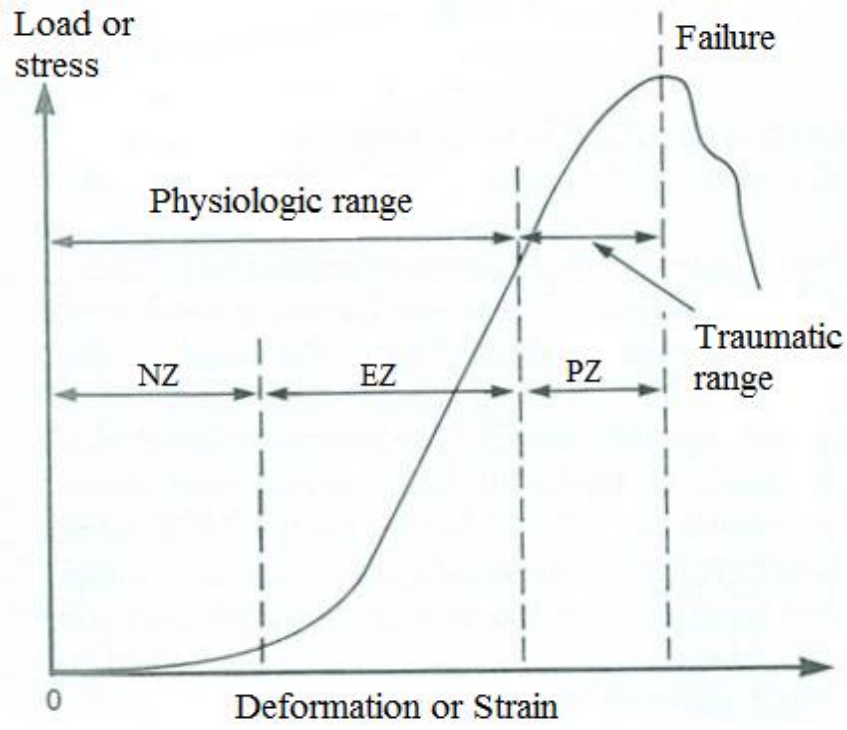

Figure 2.10: Stress strain curve of the ligament **[6]**

The ligaments exhibit nonlinear stress strain behavior as shown in figure 2.10. In physiology range, the stiffness in the neutral zone is relative smaller than in the elastic zone. If the ligament's strain goes into traumatic range, it will have plastic deformation [6].

2.4. Low Back Pain Disorders and Treatments

Low back pain is a major health problem worldwide at any age, but especially at an elderly age. The cause of low back pain is patient specific and highly variable and may be due to several different disease states. Major causes of low back pain are herniated discs, disc degeneration, spinal stenosis, and facet joint degenerations.

Several factors that might cause degeneration are: aging, mechanical factors due to occupational exposure [31-32], abnormal loading conditions [33] and the loss of nutrition to the disc. The annulus begins to tear radially and separate from the vertebral body due to stoppage of the cellular activity. Disc bulging may occur due to decrease in the radial tensile strength of the annulus. The disc also gets thinner as one

ages due to a loss of water content causing a decrease in disc height. The material properties of the disc nucleus pulposus shift from “fluid like” to “solid like”. A degenerated disc causes compression of exiting nerve roots to result in pain. Herniated discs are produced as the disc starts to degenerate and this causes the posterior disc to bulge out and decrease in height. Narrowing of the spinal canal due to annulus bulging is called spinal stenosis. Spinal stenosis has potential to cause back pain [34]. Significant pain begins in the low back and radiates down the buttocks and is worsened by walking, exercising, or standing for persons suffering from spinal stenosis [7, 35]. Pain relief is often felt by sitting, leaning forward, or squatting [7, 35]. Facet hypertrophy may cause nerve root irritation due to projection of the facet into the spinal canal, thereby compressiong nerves[6].

In the initial stages of the low back pain, doctors choose conservative treatments, non invasive technique, like traction, exercise, heat therapy or the mobilization of the joint. Surgical treatment is recommended for a patient if the pain persists even after 6-12 months of conservative treatment. The aim of surgical treatments is to remove the pain causing structures, to stabilize the segment, and to correct the bone failure due to trauma or disease. Surgical treatments include decompression surgery, fusion, and non fusion surgery.

In decompression surgery, a small part of lamina above nerve root (laminectomy), spinous process, facets (facetectomy), ligaments, and sometimes part of the intervertebral disc is removed to give more room for the nerves. Clinical studies have shown that decompression surgery enhances neurological recovery, pain relief, and mobility [36-37]. However, significant destabilization of the spinal motion segment is seen after decompression, especially if the facet joint is removed [38-39]. Postoperative movements in forward bending and axial rotation are discouraged after a decompression surgery due to a decrease in spinal stability [40]. In a finite element spine model, Zander et al. determined a facetectomy increases motion in rotation and annular disc stresses. After a wide laminectomy, motion increased in flexion, but little change in bending and extension was noted [40]. Therefore, fusion or non fusion surgery may be required to restore strength and stability of the lumbar spine after a decompression surgery [39, 41].

Fusion involves immobilizing one or more of the vertebrae of the spine using bone grafts or mechanical devices such as cages as a replacement for the natural intervertebral disc. Bone graft grows into the adjacent bone over the time thereby limit the motion at that segment [37]. Motion at the index level is completely restricted with the fusion device which puts additional burden on the levels above and below the index level. This causes increase in adjacent level degeneration over time [17-18]. While fusion relieves back pain early, pain is likely to return due to facet hypertrophy, facet arthropathy, spinal stenosis, osteophyte formation, and posterior muscular debilitation, as well as disc degeneration at adjacent levels to the fusion site [4]. Also, operating cost, discharge time was more for fusion. Successful fusion rates have approached 100% with the recent fusion techniques, but this has failed to reflect a comparable increase in the successful clinical outcome. A systematic review of mainly retrospective case series reported that the clinical outcomes after fusion is successful clinical outcomes ranged from with an average of around 68% [42]. Non fusion surgeries are investigated to overcome the problems of adjacent segments degeneration, low success rates, high operating costs, and postoperative complications.

2.5. Non fusion Systems

Non fusion devices are intended to restore the intersegmental motion and the natural load distribution near physiological limits. Non fusion devices can be grouped into disc replacement and facet replacement devices, and dynamic stabilization devices.

2.5.1. Total Disc Replacement and Facet Replacement Devices

The disc replacement devices are intended to restore normal mobility across degenerated disc, and restore the disc height. Disc replacement devices restore the disc height, so annulus fibers can return their natural length. Restoring loading distribution and disc height provide healing of annulus. Also, the disc replacement devices should mimic the normal spine kinematics.

Although the disc replacement devices restore normal mobility across degenerated disc and the disc height, many complications have already risen. Ooij et

al. reported anterior migration of the disc, degeneration at other levels, subsidence of the prosthesis, facet joint arthrosis, and polyethylene wear in several patients [43]. Dooris et al. investigated effect of artificial discs place on the range of motion with a finite element study. Dooris et al. determined placing the disc more posteriorly increased the range of motion in flexion up to 44% more than intact depending on the amount of annulus retained during surgery. In extension, the motion increased up to 40% more than intact when little annulus was retained [44].

A facet joint replacement is to replace the degenerative facets with an articulating prosthesis that would imitate the motion of the natural facet joint. Preliminary designs for the facet joint replacement are being developed. Since this concept is in the early stages, studies have to be taken up to understand the biomechanical issues involved in the design of facet joints [4]. Facet replacements must restore normal motion in flexion, extension, lateral bending, and axial rotation. They must perform well under shear and torsion loads and be able to bear 20 to 30% of the physiological load. The prosthesis also should be easy to place in all patients and fix to the bone to reduce the risk of loosening.

2.5.2. Dynamic Stabilization Systems

Dynamic stabilization systems are intended to maintain the intersegmental motion across implanted disc, and to restore the normal load transmission through the segment. Disc replacement and facet replacement devices restore the intersegmental motion, but fail to mimic load transmission through the segment. Therefore, a dynamic stabilization system should permit motion across the segment, and share load with the disc and the facets. The kinematic of the dynamic stabilization system might be close to intact spine kinematics if the location of axis of rotation is similar to the intact spine. In that case, the dynamic stabilization device prevents adjacent level degeneration [45].

After implanting the dynamic stabilization systems, it was hypothesized that control of abnormal motion and more physiologic load transmission would relieve pain and prevent adjacent segment degeneration. As a next step, the damaged disc may repair itself, unless the degeneration is too advanced.

The advantages of using dynamic stabilization systems over fusion and disc replacement devices are:

1- Ability to be performed posteriorly: Familiarity of surgeons with the posterior approach

2- Load sharing: This is an advantage over the total disc replacement and prosthetic disc replacement

3- Less invasive

4- Can be used with other non fusion technologies like total disc replacements and disc nucleus replacements

There are two types of dynamic stabilizations systems: interspinous based and pedicle screw based systems

2.5.2.1. Interspinous Based Dynamic Stabilization Systems

The interspinous devices are inserted between two adjacent spinous processes of the lumbar spine in a slightly flexed position. This allows nerves to get decompressed to provide relief from the pain. The implant also unloads the posterior disc and the facet joints. These devices may be used as a stand alone or along with fusion to stabilize adjacent segment [45]. These implants limit the motion in extensions. Among several interspinous devices, three interspinous devices are widely used: X-Stop, DIAM, Wallis system as shown in Figure 2.11.

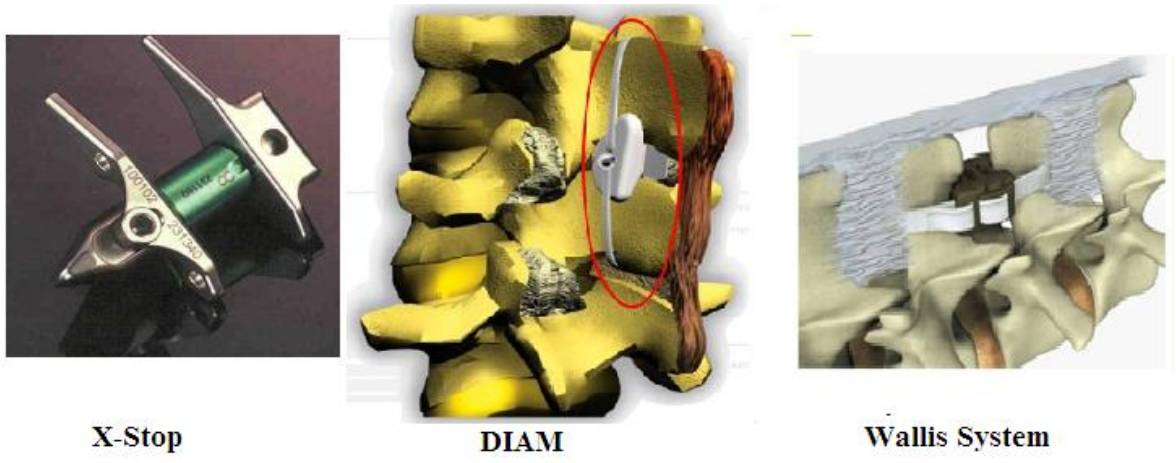

Figure 2.11: Examples of interspinous based dynamic systems [4, 46-47]

Lindsey DP et al. conducted an *In vitro* biomechanical test using seven lumbar spines to quantify the kinematics of the lumbar spine with the X-stop. The spines were tested in flexion/extension, axial rotation, and lateral bending. They found that flexion and extension range of motion was significantly reduced at the instrumented level, axial rotation and lateral bending ranges of motion were not affected at the instrumented level. They also found that the range of motion at the adjacent segments was not significantly affected by the implant [46]. Swanson KE et al. conducted a biomechanical investigation using eight cadaver lumbar specimens (L2-L5). The specimens were loaded in flexion, neutral, and extension. A pressure transducer was used to measure the intradiscal pressure and annular stresses during each of the three positions at each of the three disc levels. An appropriately sized interspinous implant (X-stop) was placed at L3-L4, and the pressure measurements were repeated. They found that the implant does not significantly change the intradiscal pressures at the adjacent levels, yet it significantly unloads the intervertebral disc at the instrumented level in the neutral and extended positions [48].

DIAM system consists of a polymeric inter-spinous spacer, with extended wings to act as a posterior shock-absorbing device. In a finite element based study of L3-S1 spine, DIAM was placed at L4-L5 level after removing the interspinous ligament. A moment of 10Nm was applied both in intact and instrumented cases. It is reported that motion at the implanted level decreased by 17% and 43% in flexion and extension respectively. There was no change in motion at the adjacent level. Intradiscal pressure at the index level was decreased by 27% in flexion, by 51% in extension and by 6% in axial rotation respectively. Adjacent level disc were unloaded by 26% and 8% at L3-L4 and L5-S1 level respectively. Motion at the implanted level decreased and no significant increase in motion at the adjacent segment was observed [47].

The Wallis system was made of PEEK composite with two attached polyester ligaments. The elastic stiffness of PEEK lies between that of the cortical bone and the cancellous. It reduces the stress that might be caused at the bone implant interface.

2.5.2.2. Pedicle Screw Based Dynamic Stabilization Systems

Pedicle screw based dynamic stabilization devices control the motion of the spine in all three dimensions of space. Pedicle screws are threaded and inserted into the pedicles. They are mainly designed to strengthen and reinforce the spine while preserving range of motion.

The Graf ligament system is one of the first dynamic implants that consist of a posterior non-elastic band to serve as a ligament between two pedicle screws (Figure 2.12). The Graf ligament was designed to control rotator movement by locking the lumbar facets in the extended position [49]. Nohara stated that restriction due to Graf ligament under flexion and bending moment is high, and the mobility of the adjacent segment is the same as the intact vertebrae [50]. Graf ligament can correct the flexion instability, but not correct the vertebral slippage.

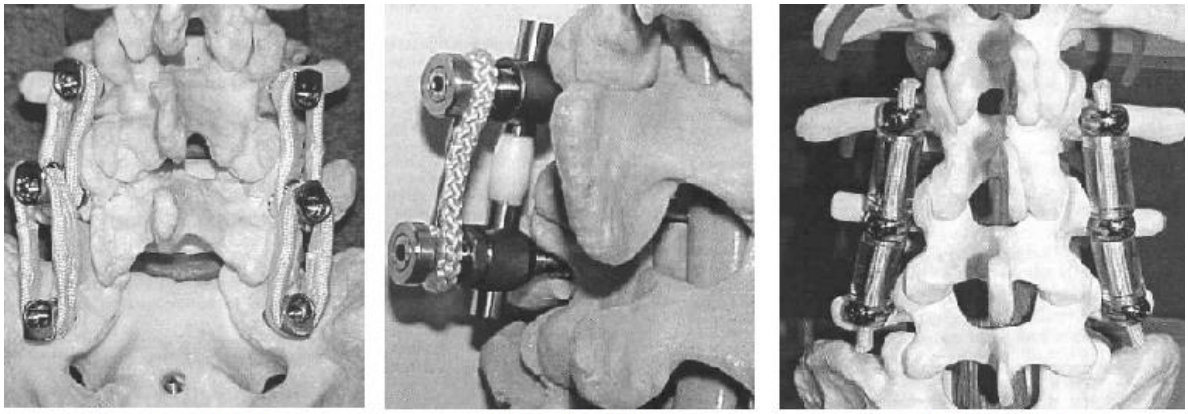

Figure 2.12: Examples of pedicle screw based dynamic stabilization systems [49, 51-52]

The fulcrum assisted soft stabilization (FASS) system was developed by Sengupta consisting of polytetrafluoroethylene fulcrums and polyurethane bands. Sengupta reported that the spine implanted FASS system has the closest load deformation curve, so the FASS system share the load with the disc and preserve the range of motion [53]. Experimental studies have shown that the implant unloads the disc, but the flexibility of the segment is lost as greater unloading of the disc occurs by the adjustment of the tension in the ligament and the fulcrum [51].

The Dynesys consists of polycarbonutethane spacers that reside between pedicle screws and a polyester cord that connects the screws. The cord controls tensile force whereas the spacer resists compressive force. Schmoelz et al. reported the degree of stabilization of the Dynesys system and the effects to the adjacent segment [53]. Eberlein determined the effect of the Dynesys on the overall stiffness with the finite element model of the L2-L3 segment [52]. Niosi et al. investigated the effect of polymer spacer length on the kinematics behavior of an implant, and described that the long spacer caused a larger range of motion in all directions [54]. The same group investigated the effect of the Dynesys system on the loading in the facet joints, and stated that Dynesys did not affect peak facet forces in extension and axial rotation, in contrast to flexion or lateral bending [55].

Rohlmann et al. studied the intersegmental rotations and intradiscal pressures in a degenerated disc after implanting the posterior dynamic implant in a finite element based study. They found that motion at the implanted level decreased and slightly increased at the adjacent level. Intradiscal pressure was also decreased at the injured level with the implant. There is no much effect on IDP at the adjacent level with the implant [56].

The Cosmic system is equipped with a hinge between the screw head and threaded portion. Cosmic is a load sharing system reducing mechanical stress on the implants (Figure 2.13). Therefore, protection against implant failure and loosening is achieved. While Dynesys stabilizes by neutralizing motion, Cosmic corrects the sagittal plane and maintains motion in flexion/extension.

Figure 2.13: Cosmic System [57]

Chapter 3 : Development of a Novel Dynamic Spinal Implant

3.1. Overview

Posterior dynamic stabilization implants are widely used to reduce loading of the intervertebral disc and facet joints for treatment of chronic lower back pain and limiting degeneration of adjacent segment with load sharing. Besides, posterior dynamic stabilization implants limit abnormal motion at the segment while preserving the motion within normal physiological limits. In the new design, Ti_6Al_4V implant rod with a helical cut and a hole at the center has controlled flexibility to preserve motion within normal physiological limits. Load sharing characteristic and motion limit of the implant depends on strength and flexibility. However, strength and flexibility, two important design objectives, may conflict with each other. Parameters that affect strength and flexibility are helical pitch, helical cut width, helical thickness, helical cut turn numbers, radial thickness, hole diameter, outer diameter are investigated to obtain both high strength and flexibility. In the investigation process, several designs are developed to investigate the effects of design parameters on strength and flexibility of implant. In each design model, only one parameter under investigation is changed within a certain range while the other parameters are kept constant. A nonlinear large deflection solution in FEM is used for every design model to determine deflection amounts and force at magnitudes when Von Misses stress reaches to 1000 MPa. In the final design, the dynamic spinal implant achieves 6.32° rotation under 100 N axial force and 4 N.m bending moment.

3.2. Introduction

Lumbar spinal fusion is a commonly used surgical treatment in disc degeneration which is related to chronic lower back pain and other spinal disorders, such as disc herniation, spondylolisthesis, facet arthropathy, and spinal stenosis [58]. Although the disc degeneration is the reason for chronic lower back pain, the primary reason for back pain is the instability of the lumbar spine [59]. However, the lumbar

instability is not defined clearly. Panjabi defines the instability as a result of failure to maintain the neutral zone in which spine motion occurs with minimal internal resistance, within normal physiological limits. The instability causes pain and abnormal motion [60]. Stokes et al. [61] and Weiler et al. [62] also related abnormal motion to chronic back pain. However, the abnormal motion, as a definition of instability, can not be explained as a cause of back pain for some cases, such as abnormal movement is observed radiological in disc degeneration with spondylolisthesis, although pain is not continuous[51]. Therefore, the definition of instability is updated to abnormal movement at the joint surface and altered load transmission [59]. The normal disc transmits load uniformly across the vertebral endplates due to isotropic property of disc consisting of homogeneous gel of collagen and proteoglycan. Disc degeneration causes the change in the isotropic property of a disc that result in uneven load transmission over the vertebral endplates. McNally and Adams claim that the pattern of loading, rather than loading value, is related to back pain [63]. Therefore, the key parameters of dynamic implants are a uniform reduction of motion to control abnormal motion at the segment while maintaining stability and uniform unloading of discs and facet joint with load sharing.

Spinal fusion restricts the motion of the affected vertebrae segment to provide stability of the spine. Boos and Webb (1997) show that although developing the fusion techniques, from pedicle instrumentation, to cage devices, and circumferential fusion devices, increased the successful fusion rates up to 98%, the clinical success does not improve [64]. Besides, the review of Cochrane database showed that spinal fusion does not make a significant improvement of history of mechanical back pain [65]. Spine fusion also affects the daily life of the patient due to a restriction of motion at the affected segment. Many studies were done in order to investigate the negative effect of fusion on the adjacent segment [66-73]. The studies show that fusion increased intradiscal pressure and mobility at the adjacent levels [66]. Rahm and Hall state that hyper mobility in the adjacent segment accelerates the degeneration in the facet joints [67]. Ahn et al. compared the load sharing characteristics of rigid and dynamic rod devices, and showed that a dynamic implant can reduce stress shielding by load sharing which could slow degeneration [74]. Meyers et al. examine the effects of a different design approach in dynamic implant,

Dynesys system and Total Posterior Spine (TOPS) Systems on the load sharing of the posterior column and disc [75]. Meyers et al. stated that the moments in the screw with the Dynesys System were higher that with the TOPS System as much as %56 in flexion extension and %86 in lateral bending. He concludes that different design approach influenced the load sharing of the posterior column and disc.

Although considerable research has been devoted to the biomechanical effects of the dynamic spine implant, such as load sharing and stabilization, there is little research about the optimum design of the dynamic spine implant. The optimum design is a balance between strength and flexibility. Strength provides load sharing and stabilization capabilities of an implant whereas flexibility preserves the motion within normal physiological limits. Helical cuts are created into a rigid rod to give limited flexibility to preserve motion within normal physiological limits. In the design, investigation parameters that affect load sharing and flexibility are helical pitch, helical cut width, helical width, helical cut turn numbers, radial thickness, hole diameter, outer diameter.

3.2. Materials and Methods

The new dynamic implant consists of main body part that provides flexibility to the implant and two 6 mm rigid rod parts that are assembled to the main body part with thread (Figure 3.1). Implantation is simple and similar to pedicle screw/rod implantation because after the pedicle screws are inserted to vertebra, the locking screws engage with the rod part of the implant just like pedicle screw/rod implantation. The new dynamic implant must be oriented such that starting and finishing points of helical cut must lie on the sagittal plane. Helical cut is created within main body part to give flexibility that allows motion in the flexion, extension, and lateral bending. A hole is inserted to the main body of implant to help flexibility. The flexibility basically depends on helical cut width, helical width, radial thickness, helical cut turn number. (Figure 3.1) Radial thickness is half of the difference between outer and inner diameter of the main body part. The sum of helical cut width and helical width gives helical pitch.

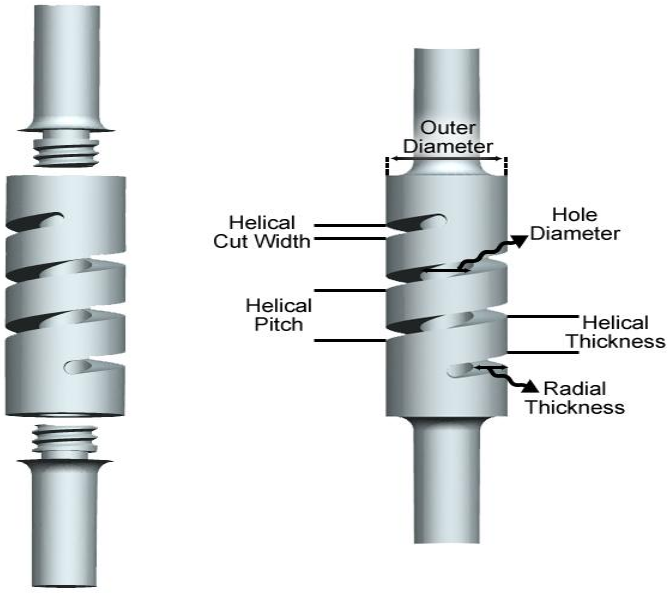

Figure 3.1: The part of implant and parameters

Flexibility and strength are two key parameters that determine performance of the dynamic spinal implant. Strength gives compressive stiffness to unload the intervertebral disc and the facet joints across affected segment with load sharing. The balance between flexibility and strength provide load sharing capability that prevents adjacent segment degeneration, and preserves the motion within normal physiological limits. Therefore, the following parameters that affect load sharing and flexibility were investigated to construct the balance: helical pitch, helical cut width, helical width, helical cut turn numbers, radial thickness, hole diameter, outer diameter.

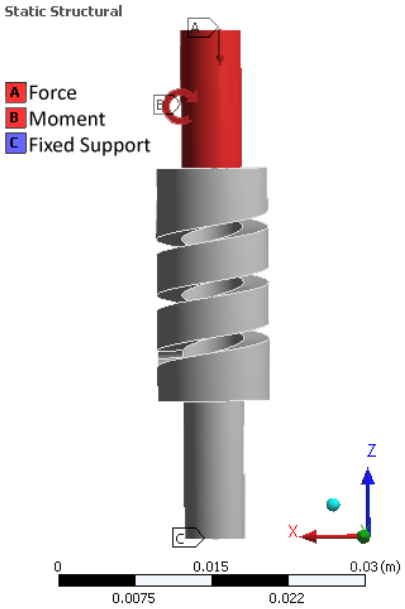

Figure 3.2 : The fixation and loading points of the implant

In the investigation process, several models were developed to determine effects of parameters on implant strength and flexibility. Only the parameter under investigation was changed within a certain range while other parameters are kept constant. A nonlinear analysis technique was used in ANSYS 11.0 with 1.5 mm element size and SOLID185 element type for every model to provide sufficient accuracy. Amount of deflection and von Misses stresses were investigated for every model. According to ASTM F1717, the perpendicular distance to the applied load between the insertion point of an anchor and the load application center is 40 mm, therefore in the analysis the compressive force was applied in z direction, and moment was is loaded around y axis. Applied moment was the product of 40 mm moment arm times the magnitude of applied force. The details of fixation points and loading points can be seen in the Figure 3.2. The implant was made of Ti_6Al_4V with 115 GPa elastic modulus and 0.36 poison's ratio. Yield and ultimate stresses of Ti_6Al_4V are 1030 MPa and 1150 MPa, respectively. The models were compared according to their loading value and total deformation at the 1000 MPa Von Misses stress. Several design models which have different parameters were manufactured. Some of these models are shown in Figure 3.3. Experimental and FEM results for

axial and bending stiffness of the produced examples are close as can be seen in Table 3.1.

Figure 3.3: Photograph showing a series of produced dynamic spinal implants

Table 3.1: Axial and bending stiffness of examples

Model	Experimental & Finite Element Analysis (FEM)	Axial (N/mm)	Bending (N/mm)
M 58	Experimental	376.9	25.4
	FEM	380	27.3
M 59	Experimental	200.5	16.15
	FEM	210.9	18.53
M 60	Experimental	33.76	3.6
	FEM	39.9	3.9
M 61	Experimental	752	40
	FEM	817.4	39.7

3.3. Results

3.3.1. Effect of Pitch on Strength and Flexibility

In the research, pitch that is composed of cut width and helical thickness was changed between 3.478 mm and 8.478 mm with several cut width and helical thickness combinations while radial thickness (3.475 mm), hole diameter (4 mm), outer diameter (10.95 mm), number of helical cut turn (2 turns) were kept constant. The investigation about the pitch effect on the strength and flexibility brought the general idea of strength and flexibility behavior of several cut width and helical thickness combinations.

Table 3.2: Parameters of the pitch effect investigation

Model	M 1	M 2	M 3	M 4	M 5	M 6	M 7	M 8	M 9
Pitch [mm]	3.478	3.478	4.250	4.478	5.478	5.478	6.478	7.478	8.478
Cut width [mm]	2.500	1.500	2.250	1.600	2.250	1.800	2.000	2.000	4.000
Helical Thickness [mm]	0.978	1.978	2.000	2.878	3.228	3.678	4.478	5.478	4.478

It should be noted that 50 N force in graphs means 50 N axial force along z and 2 N.m (50Nx40mm) moment around y axis. Table 3.2 and Figure 3.4 illustrate that comparison of Model 1 and Model 2. They have same pitch, but Model 2 has bigger helical thickness. This comparison emphasized that increasing helical thickness improves strength of implant and decreases the flexibility if helical thickness is considerably small respect to cut width. In contrast, comparison of Model 5 and Model 6 underlines that increasing helical thickness improves strength, not as significant at the Model 1 and Model 2, and increases flexibility due to high ratio of helical thickness and cut width. Model 2 and Model 3 has same helical thickness, but different cut width. Comparison of Model 2 and Model 3 illustrates that both strength and flexibility decreases as cut width increases. Comparisons of the set of Model 3 and Model 5 and the set of Model 7and 8 respectively demonstrate that increasing of helical thickness as cut width is kept constant causes improvement of both strength and flexibility. Investigation of pitch effects served as a guideline for strength and flexibility behavior of cut width and helical thickness combinations.

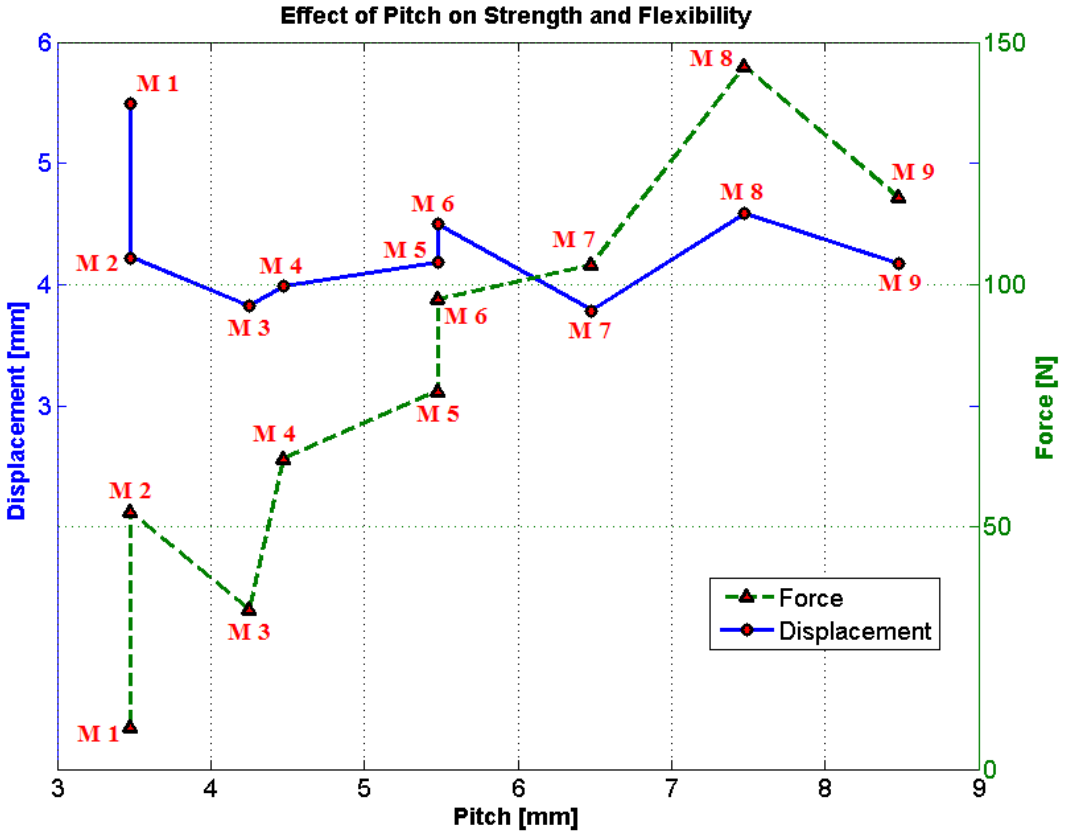

Figure 3.4: Effect of pitch on strength and flexibility

3.3.2. Effect of Helical Thickness on Strength and Flexibility

In the investigation of effect of helical thickness on strength and flexibility, pitch was kept constant at 5.478 mm while cut width was changed between 4.5 mm and 1.0 mm, conversely helical thickness was changed between 0.978 mm and 4.478 mm. In this investigation, radial thickness (3.475 mm), hole diameter (4 mm), outer diameter (10.95 mm), and number of helical cut turn (2 turns) were kept constant. As can be seen in Figure 3.5, strength was improved, but flexibility decreased as helical thickness was increasing up to Model 15. After Model 17, both strength and flexibility improved as helical thickness was increased. Figure 3.5 and Table 3.3 illustrate that if the ratio which is helical thickness over cut width is significantly small, strength increases, but the flexibility decreases as the helical thickness increases because the structure of implant becomes more stable. As the ratio is getting closer to one, flexibility is constant while helical thickness increases. After

this region, flexibility is improved as helical thickness increases if ratio is getting bigger.

Table 3.3: Parameters of the helical thickness effect investigation

Model	Cut width [mm]	Helical Thickness [mm]
M 10	4.50	0.978
M 11	4.25	1.228
M 12	4.00	1.478
M 13	3.75	1.728
M 14	3.50	1.978
M 15	3.25	2.228
M 16	3.00	2.478
M 17	2.75	2.728
M 18	2.50	2.978
M 19	2.25	3.228
M 20	2.00	3.478
M 21	1.75	3.728
M 22	1.50	3.978
M 23	1.25	4.228
M 24	1.00	4.478

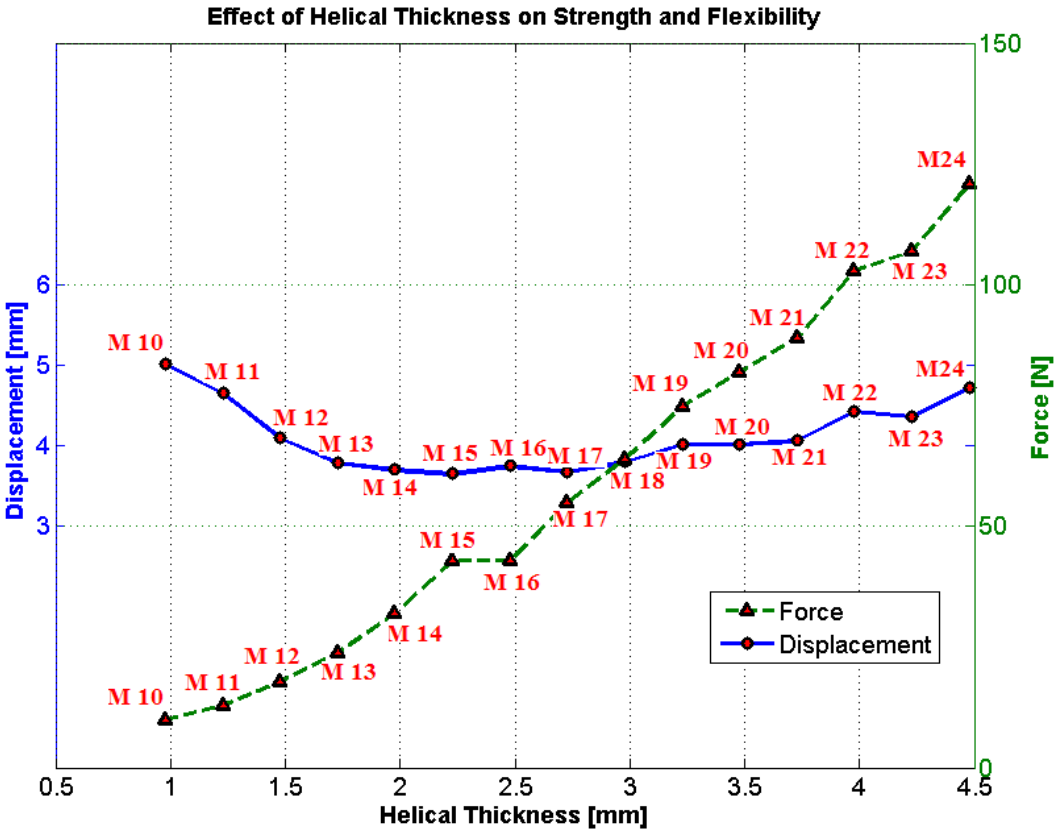

Figure 3.5: Effect of helical thickness on strength and flexibility

3.3.3. Effect of Radial Thickness on Strength and Flexibility

In the investigation of radial thickness effect on strength and flexibility, pitch (5.478 mm), and hole diameter (2 mm), helical thickness (2.978 mm), cut width (2.5 mm), and number of helical cut turn (2 turns) were kept constant, while radial thickness was changed between 6.0 mm and 1.0 mm. Radial thickness was increased with outer diameter. Outer diameter was changed from 14.0 mm to 4.0 mm. Figure 3.6 presents that increasing of radial thickness has a positive effect on flexibility and strength of the implant.

Table 3.4: Parameters of the radial thickness effect investigation

Model	M 25	M 26	M 27	M 28	M 29	M 30	M 31	M 32	M 33	M 34
Radial Thickness	1.00	1.50	2.00	2.50	3.00	3.50	4.00	5.00	5.50	6.00
Outer Diameter	4.00	5.00	6.00	7.00	8.00	9.00	10.00	12.0	13.0	14.0

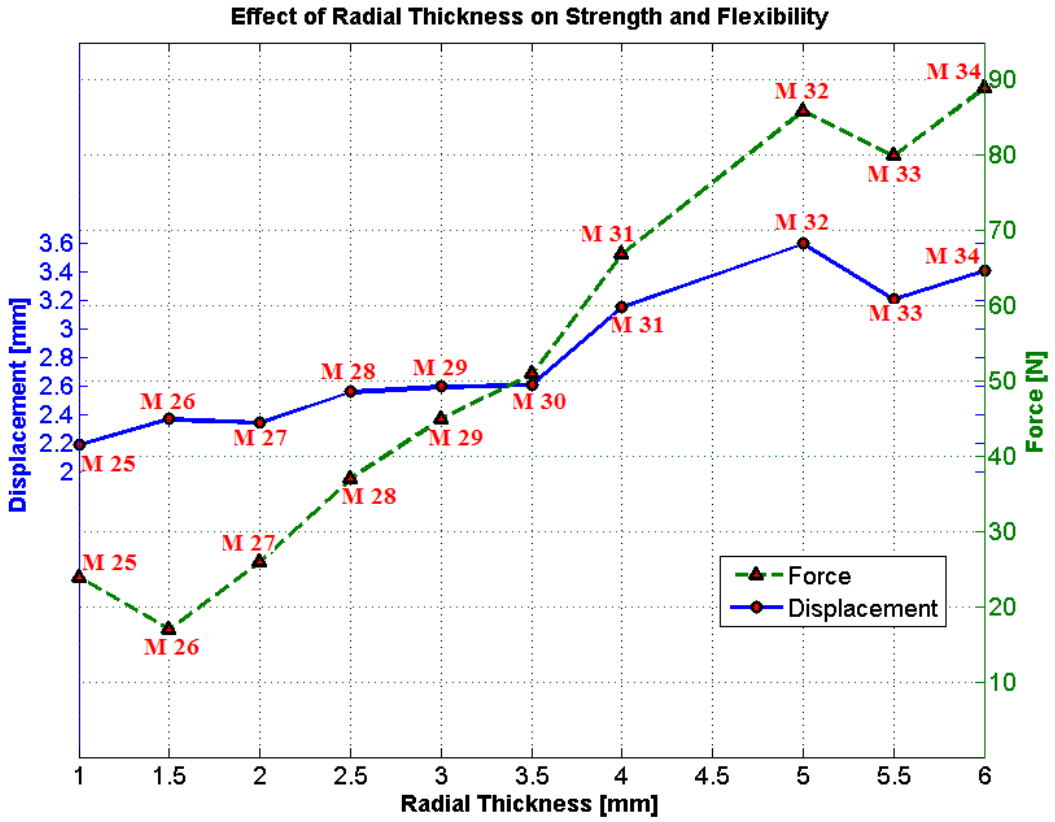

Figure 3.6: Effect of radial thickness on strength and flexibility

3.3.4. Effect of Hole Diameter on Strength and Flexibility

As can be seen in Table 3.5, pitch, cut width, helical thickness, outer diameter, and number of helical cut turn were kept constant at 5.478 mm, 2.5 mm, 2.978 mm, 10.95 mm, and 2 turns respectively, while hole diameter was changed between 2.0mm and 6.0 mm. Radial thickness changed depending on the hole diameter. Figure 3.7 shows that as hole diameter increases strength of implant decreases, but flexibility increases. However, the trend is not clear especially for strength. Besides, the results conflict with radial thickness effect because flexibility increases as radial thickness decreases.

Table 3.5: Parameters of the hole diameter effect investigation

Model	M 35	M 36	M 37	M 38	M 39	M 40	M 41	M 42	M 43
Hole Diameter	2.0	2.5	3.0	3.5	4.0	4.5	5.0	5.5	6.0
Radial Thickness	4.475	4.225	3.975	3.725	3.475	3.225	2.975	2.725	2.475

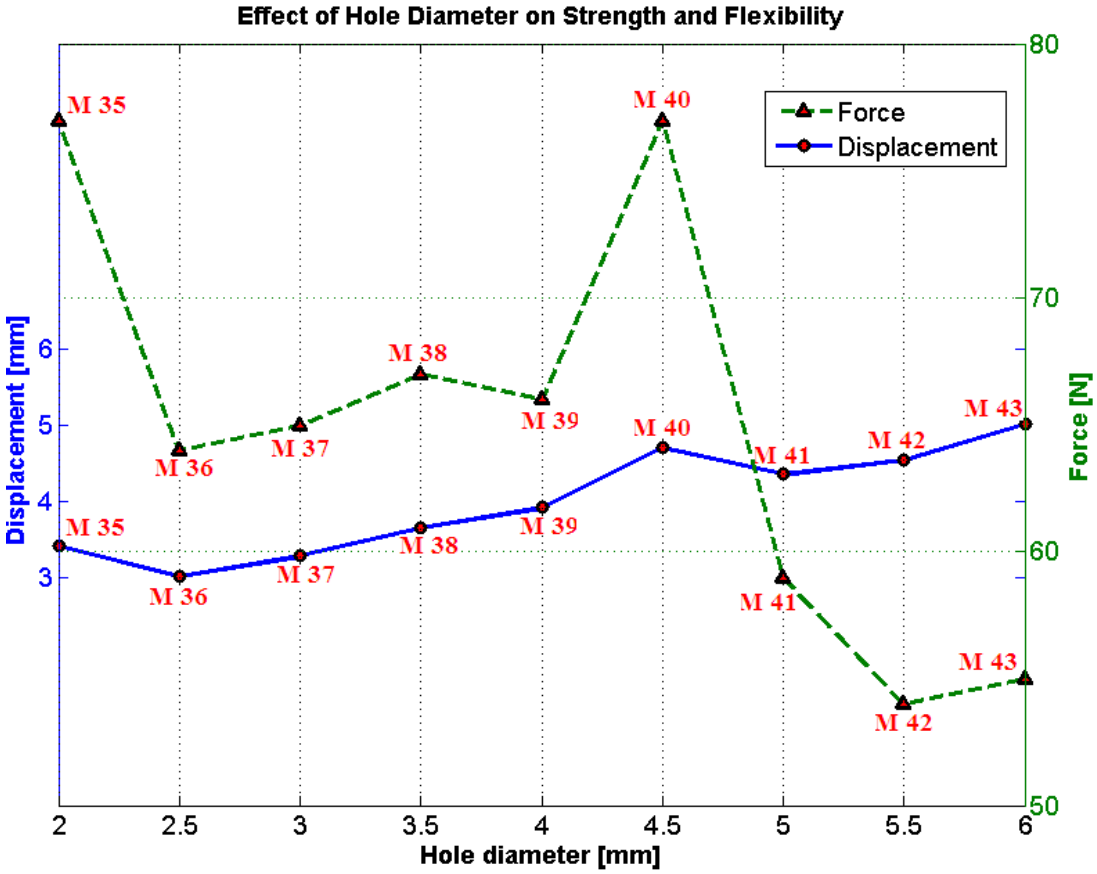

Figure 3.7: Effect of hole diameter on strength and flexibility

3.3.5. Effect of Cut Turn Number on Strength and Flexibility

As can be seen in Table 3.6, only helical turn number was changed from 1 to 5 with various steps. Pitch, cut width, helical thickness, radial thickness, hole diameter, and outer diameter were kept constant at 4.478 mm, 1.6 mm, 2.878 mm, 3.475 mm, 4.0 mm, and 10.95 mm, respectively. Figure 3.8 illustrates that cut turn number increase from 1 turn to 1.25 turn, the strength of the implant becomes weaker rapidly. However, after that point the strength did not change significantly although flexibility has a positive trend with turn number. This result is crucial for the study

because the model with high pitch value that has high strength but low flexibility was chosen firstly. Then, cut turn number was increased to improve flexibility of the implant.

Table 3.6: Parameters of the cut turn number effect investigation

Model	Turn number	Model	Turn number
M 44	1.00	**M 51**	3.00
M 45	1.25	**M 52**	3.25
M 46	1.50	**M 53**	3.50
M 47	2.00	**M 54**	3.75
M 48	2.25	**M 55**	4.00
M 49	2.50	**M 56**	4.50
M 50	2.75	**M 57**	5.00

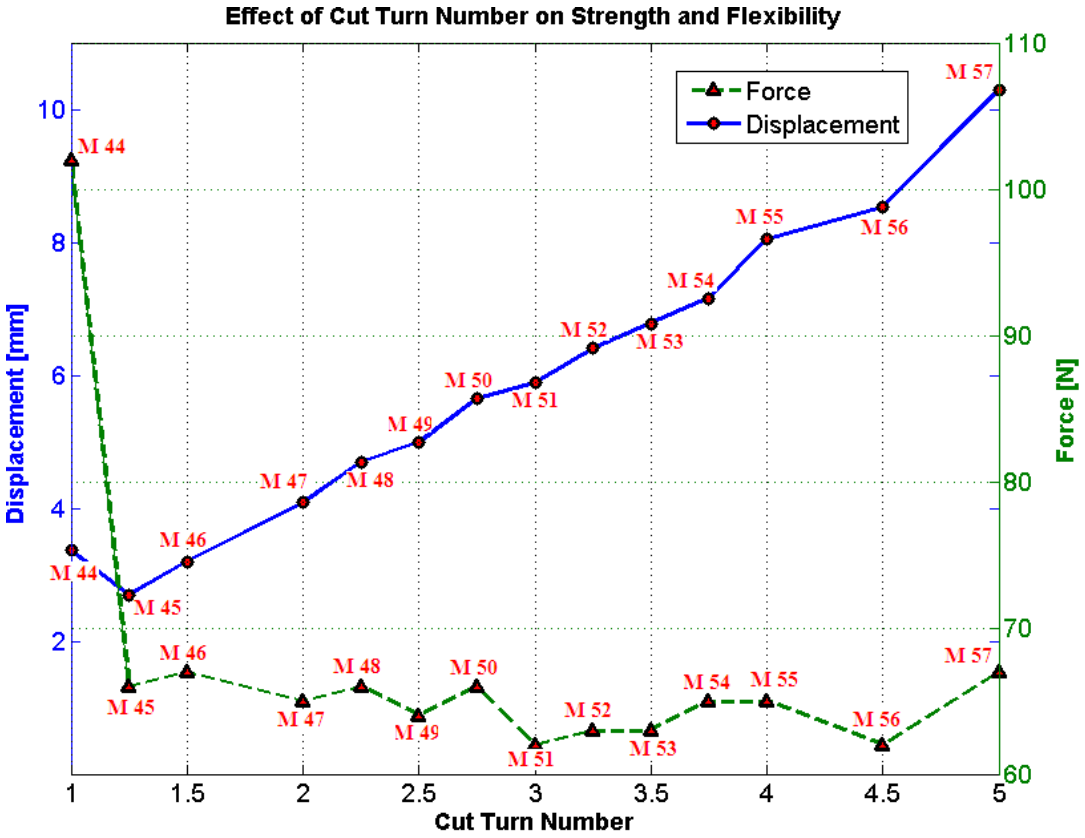

Figure 3.8: Effect of cut turn number on strength and flexibility

3.4. Discussions

The investigation of pitch effect on the strength and flexibility brought the general idea of strength and flexibility behavior of several cut width and helical thickness combinations. One of the significant results from this investigation is that if helical thickness is considerably small respect to cut width, increasing helical thickness improves strength of implant and decreases the flexibility. In contrast to that, due to high ratio of helical thickness and cut width, increasing helical thickness again improves strength, not as significant at the Model 1 and Model 2, but increases flexibility at this time. Another result of this investigation is that both strength and flexibility decreases as cut width increases if helical thickness is same. In addition to these, increasing of helical thickness as cut width is kept constant causes improvement of both strength and flexibility.

Helical thickness effect was explained in three regions. If the ratio of helical thickness over cut width is significantly small, strength increases, and flexibility decreases as helical thickness increases. As the ratio is getting closer to one, the flexibility is constant while strength increases. After this region, both flexibility and strength are improved as helical thickness increases. Although the trend is not clear especially for strength, as hole diameter increases strength of implant decreases, but flexibility increases. It was seen that the strength of the implant becomes weaker rapidly if cut turn number increase from 1 turn to 1.25 turn. After that point, the strength did not change significantly although flexibility has a positive trend with turn number.

In the investigation process, 7.478 mm pitch was chosen due to its high strength. Although several combinations were considered, its flexibility could not be improved to higher level. Therefore, pitch value was reduced step by step, and several combinations were built for a certain pitch value. Model with 5.478 mm pitch that composed of 1.5 mm cut width and 3.978 mm helical thickness, 6 mm hole diameter, 10.95 mm body diameter, and 3 turn gave the best strength over flexibility ratio. The chosen implant undergoes 6.32° rotation under 100N axial force and 4 N.m bending moment. Bending and axial stiffness of the chosen implant are 39.7 N/mm and 817.4 N/mm, respectively.

3.5. Conclusion

Performance of the implant is directly related to its flexibility and strength. Strength provides compressive stiffness to unload the intervertebral disc and the facet joints across affected segment with load sharing. Flexibility and strength must be in balance to get maximum performance from the implant. Therefore, the following parameters that affect load sharing and flexibility were investigated to construct the balance: helical pitch, helical cut width, helical thickness, helical cut turn numbers, radial thickness, hole diameter, outer diameter. A novel dynamic spinal implant with desired strength and flexibility was designed.

Chapter 4 : Development of Finite Element Model

4.1. Overview

In recent years, many FEA models have successfully modeled the human spine, so they provide insights into spine biomechanics. Newly created implants can be adapted to better match the mechanical characteristics of actual tissue before it is prototyped [22-23]. Finite element analysis allows researchers to repeat experiments, change parameters, so analyze the effect and influence of a single entity within a complex assembly to provide valuable insights into a wide range of situations.

In spine biomechanics, finite element analysis helps to understand how newly created implant affects the kinematics of spine such as segmental motion, adjacent level effects, facet contact patterns. Also, it is possible to obtain information that is not accessible through experimentation, such as the stress distribution through the intervertebral disc. As well as for intact spine, finite element modeling can be a valuable tool in simulating biomechanical features of spine in its injured and surgically altered states.

In finite element modeling, the spine has nonlinear properties containing the material nonlinearity, geometric nonlinearity, and boundary nonlinearity. The contact reaction of facets causes the boundary nonlinearity. The ligament, annulus disc, nucleus pulposus material behavior are some of the material nonlinearities. The geometric nonlinearity is occurred due to large displacement formulation.

This chapter begins with a brief literature review. The chapter describes detailed explanation of each step in development of finite element model of L3-L4 spine segment. Both creation of each FSU part geometry and material behavior definition of each FSU part are explained.

4.2. Literature Review

Numerous FE analyses have been made on the clinical biomechanics of the lumbar spine. Goel and Kim [1989] studied total denucleation in the intact model and in a model with bilateral total discectomy using L3-L4 segment with sagittal plane symmetry [76] . It was reported that facets played an important role in protecting the injured disc and the load born by this structure increased by 80% after denucleation. However, vertebral body stresses did not increase significantly and disc bulge decreased.

The annulus failure initiation and propagation were studied under the different load cases by Natarajan et al with intact and damaged L3-L4 segment. Natarajan et al. reported that failure always started at the endplate indicating that this zone is weak link of the body-disc-body unit. Compressive load are not expected to produce failure in the annulus failure, but in the endplate [77].

Goel et al. also investigated the differences provided by the model of a ligamentous L3-L4 segment with the muscles effects both considered and ignored. It was shown that the muscles provided more stability to the ligamentous model, decreased the stresses within the anterior column and increased the load share of the articular facets [78]. Zander et al. investigated effects of the bone graft size, placement, and stiffness on the lumbar spine biomechanics using L1-L5 spine model with internal fixator and interbody bone graft at the L2-L3 level. It was concluded that stresses in the endplates adjacent to bone graft increased. Overloading increased with bone graft stiffness. Large grafts with low stiffness should biomechanically be preferred [40].

Eberlein et al. studied on L2-L3 lumbar spine with Dynesys implant. He compared range of motion with the implant with or without nucleusectomy. Great stiffening effect of the device on the motion segment and non physiological biomechanical response in axial rotation were reported [52]. Rohlmann et al. modeled disc degeneration effect on range of motion, intradiscal disc pressure, and facet joint forces. Due to disc height reduction, annulus fibrosus stress and facet joint force increased with disc degeneration. However, as ranges of motion decreased with

the grade of degeneration, facet joints increase was not proportional to degeneration degree [56].

4.3. Building Geometry

The first step of finite element modeling is construction of geometry. In this study, computer tomography (CT) images were utilized to create spine geometry. CT images provide information about geometry of bone. Gained information had helped to overcome some of the problems of registering the complex geometry of the spine. Despite advantages of utilizing CT images to create spine geometry, there are several disadvantages that can result in a loss of geometric quality. A common limitation is the use of relatively thick CT image slices. Therefore; to ensure optimal segmentation of the data, CT studies should be acquired as thin axial slices, using high kV and reconstructed using a sharp filter.

The CT data used in this study were that of a 21-years-old female subject, acquired using axial slices 0.488mm thick, at 120kV and reconstructed using a bone filter algorithm. Each slice had 512x512 pixels in 16 bit depth grayscale. 681 CT images were used to create the lumbar spine geometry. The CT study was reviewed by Clinical Specialists at American Hospital to eliminate any obvious defects in the lumbar spine, which might cause detrimental effects in the modeling of a healthy spine. All lumbar vertebrae, intervertebral discs, and facet joints were modeled in the commercially available software Mimics 13.1. The workflow is as follows:

1- Data import
2- Image Segmentation
3- Manual correction
4- Image segmentation for soft tissue
5- Stack 2D boundaries into 3D surface
6-Export 3D surface of vertebra to Remesh module
7- Export intervertebral disc to Hypermesh

4.3.1. Data Import

The CT images were transferred from the database in DICOM format. Using import functions, these DICOM images were loaded and calibrated for voxel size. Figure 4.1 illustrates the data after importing.

Figure 4.1: Data after importing CT images

4.3.2. Image Segmentation

Segmentation assigns labels to the individual voxels in the image to identify the different structures within the volume data set. As a first step in segmentation, a profile line was drawn from soft tissue to the bone. Along this line an intensity profile line was generated.

According to the intensity profile, start and end value of thresholding were determined. A low threshold value makes it possible to select soft tissue of the scanned patient. With a high threshold, only the very dense parts remain selected, such as bone. After thresholding, the segmentation object contains only those pixels of the image within threshold boundaries. In this study, lower threshold is 180, whereas higher threshold is 2976 Hounsfield value for bone structures. Techniques of thresholding and region growing were used to distinguish bone from other tissues. The region growing tool makes it possible to split the segmentation created by thresholding into several objects and to remove floating pixels. In the region growing, one point of the interested object is selected. All points in the current segmentation object that are connected to the marked point will be moved to the target mask. Figure 4.2 illustrates the data after automatic segmentation.

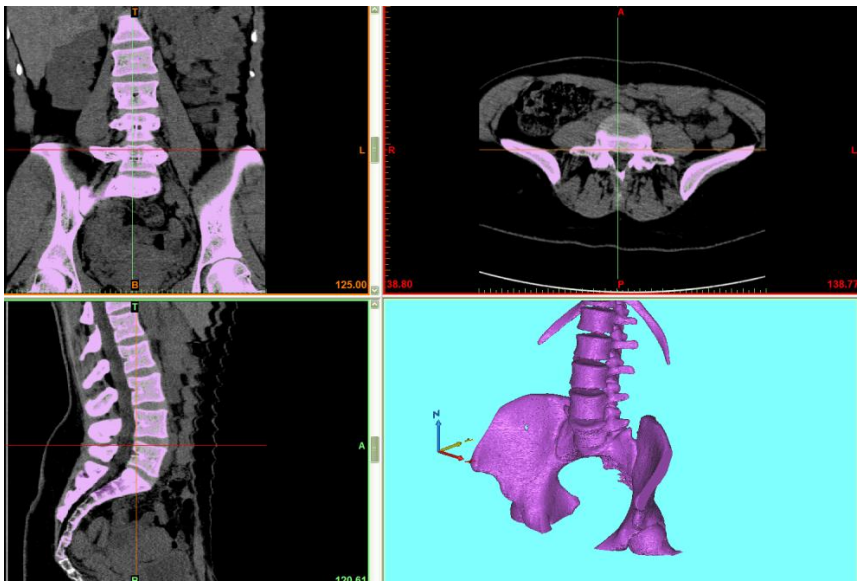

Figure 4.2: Image segmentation

4.3.3. Manual Correction

While using high dose and a sharp filter provides for accurate geometry, it introduces noise in the image. To remove the noise and surrounding tissues that might have been introduced due to a low threshold, manual segmentation was performed. As can be seen in Figure 4.2, all lumbar vertebrae are one part. A small part of the cartilage of facets was erased to separate each vertebra apart, as shown at upper right window in Figure 4.3. After each lumbar segment was separated, each segment was divided into five parts with manual operation according to Hounsfield value. These parts are cortical bone, cancellous bone, posterior bone, upper endplate, lower endplate, as shown at lower right window in Figure 4.3. At the end of this step, final segmentation of each facet joints and each vertebra with subparts were created. Figure 4.3 illustrates the data after semiautomatic and manual segmentations.

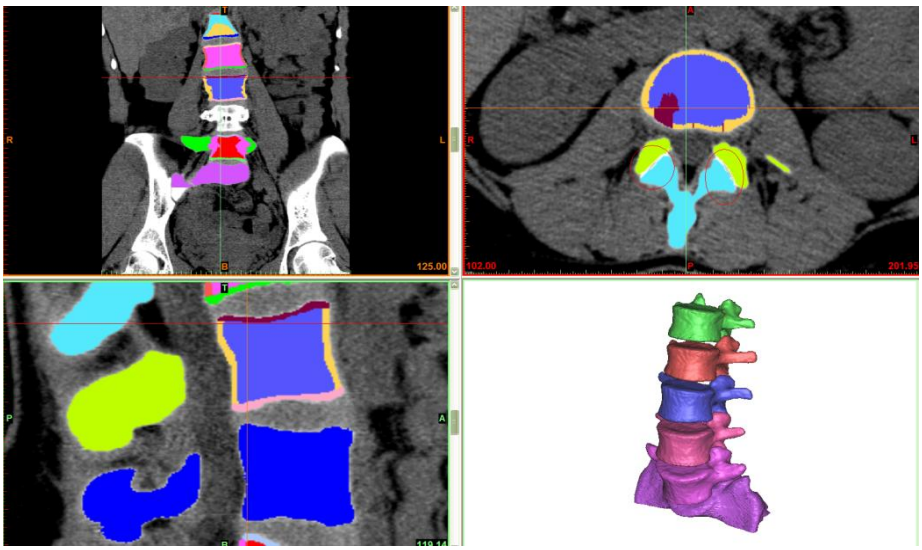

Figure 4.3: The data after semiautomatic and manual segmentations

4.3.4. Image Segmentation for Soft Tissue

Final segmentation of each facet joints and each vertebra with subparts were created at the end of manual correction step. At this step, creation of the intervertebral disc geometry will be explained. New profile was drawn for soft tissue. According to the new intensity profile, start and end value of thresholding were determined for intervertebral disc. Lower threshold is -75, whereas higher threshold is 1442 Hounsfield value. After thresholding, new segmentation object contains only intervertebral disc with a lot of noise. Techniques of region growing were used to distinguish each disc from each other. To remove the noise, manual segmentation was performed. Figure 4.4 illustrates intervertebral disc masks and L3-L4 segment geometry.

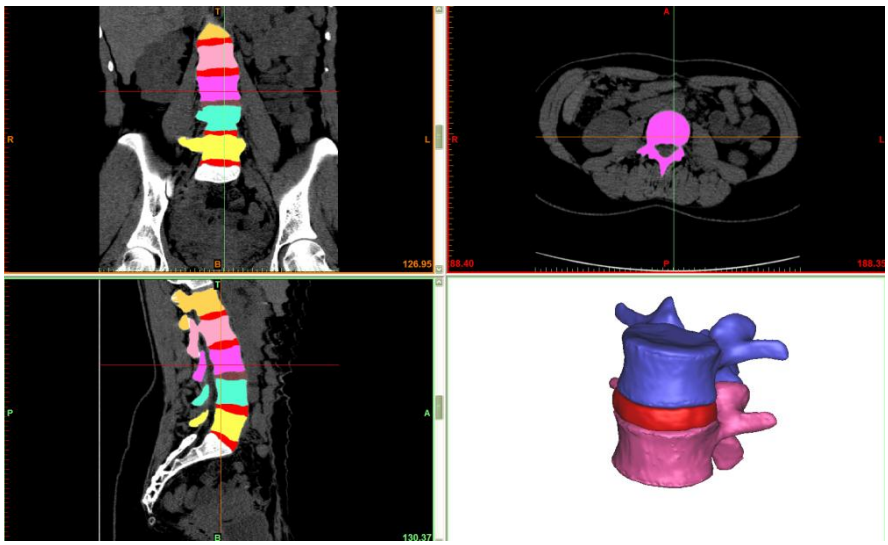

Figure 4.4: Intervertebral disc masks and geometry of L3-L4 segment

4.3.5. Stack 2D Boundaries into 3D Surface

Using polygon post-processing tools, surfaces were generated for the 3-D volume. These volumes were visualized using rendering techniques which allow for direct visualization of the 3-D data using a physically-based light emission / absorption model as illustrated in Figure 4.5.

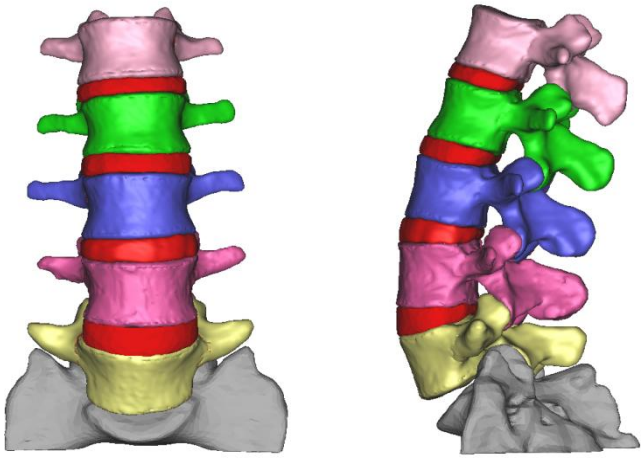

Figure 4.5: 3-D model of lumbar spine

4.3.6. Export 3D Surface of Vertebra to Remesh Module

Newly created 3D surfaces of vertebrae were exported to Remesh module to create tetrahedron mesh. Depending on the parameters for 3D calculation, the resulting 3D surfaces included too much detail. In Remesh module, as a first step, the

amount of detail was reduced by applying a smooth to the 3D surfaces. In smoothing operation, 1st order Laplacian method with 0.7 smooth factor and 10 iterations was used. As s second step, the amount of triangles was reduced. In reduction operation, normal method with 15° flip threshold angle and 10 iterations were used. In this study, the Height/Base (N) shape parameter was used to measure the quality of the triangles. This parameter measures the ratio between the height and the base of a triangle and normalizes the value. A perfect equilateral triangle has a quality of 1 and a very bad triangle has a quality of 0. To improve the quality of triangles, auto remesh was made with 0.4 quality threshold, 0.2 geometric error, 4 iterations, and 5 maximum edge length parameters. In order to get a more uniform mesh, maximum edge length was limited. Next step was quality preserving triangle reduction. As a last step, surface mesh consisting of triangles was converted to volume mesh consisting of tetrahedron elements. Figure 4.6 illustrates volume mesh of L3 vertebra.

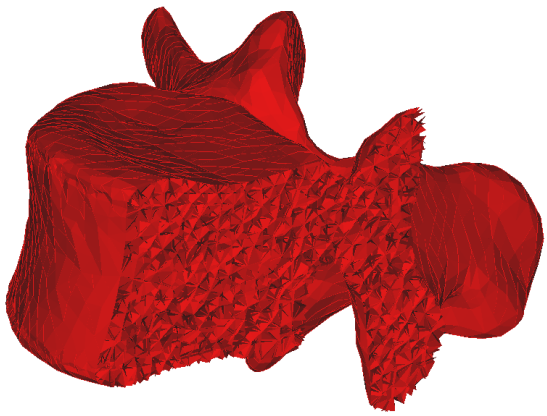

Figure 4.6: Volume mesh of L3 vertebra

4.3.7. Export Intervertebral Disc to Hypermesh

Intervertebral disc is comprised of two distinct components: the central nucleus pulposus and the periphery annulus fibrosus. Whole IVD geometry was created at the end of soft tissue segmentation at third step. At this step, IVD was divided into the annulus fibrosus and nucleus pulposus, and then annulus fibers were created.

IVD was divided into the annulus fibrosus and nucleus pulposus in Mimics program with cutting orthogonal to screen tool. In this study, the nucleus pulposus covers approximately 45 % of the cross sectional area of whole IVD. Original IVD was rescaled with appropriate constant, so rescaled IVD was approximately 45 % of the cross sectional area of original IVD. Then, a cutting line that follows circumstance of rescaled IVD was drawn. According to this line, original IVD was divided into the annulus fibrosus geometry and nucleus pulposus geometry.

In this study, the annulus fibrosus has 8 concentric layers of fibers from the innermost to the outermost boundary of the disc. The direction of fibers in each layers typically alternately from approximately +/- 30°. To create 8 concentric layers, geometry of annulus fibrosus were divided into three parts with previously explained steps.

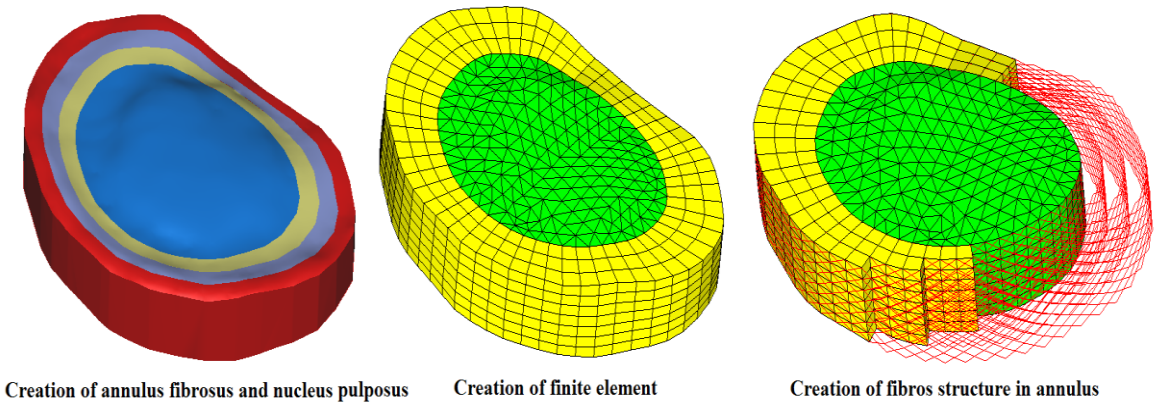

Figure 4.7: The development of annulus fibrosus and nucleus pulposus

The geometries of the annulus fibrosus' part and nucleus pulposus were exported to Hypermesh with STL format. In Hypermesh, the annulus fibrosus was meshed with hexahedral elements, whereas the nucleus pulposus was meshed with tetrahedral elements. Finally 8 layers of fibers were created with truss elements. Figure 4.7 illustrates annulus fibrosus, nucleus pulposus, and 8 layers of fibers.

4.4. Vertebrae

Finite element meshes of vertebrae were created in Mimics. Boundaries of cortical, posterior, and endplates were determined with utilizing CT images. In contrast, the majority of studies assumed thickness of cortical and endplates as a constant value. For instance, the thickness of cortical bone is 0.35mm in Guilhemm [79], 0.4mm in Pitzen [80], and 1.0 mm in Tian-Xia [81] studies. Therefore, this study is more accurate representation of vertebrae.

Finite element meshes of vertebra were exported to Hypermesh with Abaqus format. Figure 4.8 illustrates mesh of L3 vertebra with 5 different bony structures in Hypermesh. All of the bony structures were meshed with C3D4 elements. The cortical bone and endplates are modeled generally with hexahedral or shell elements, while posterior and cancellous bones are modeled with hexahedral elements.

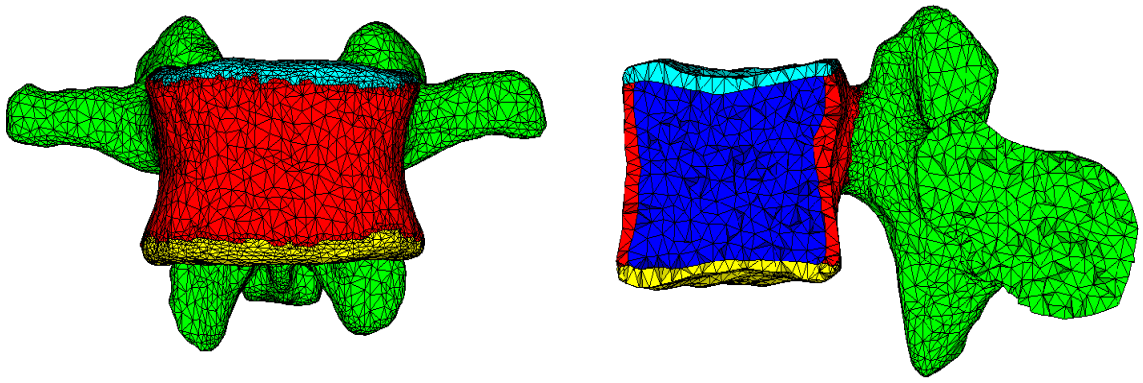

Figure 4.8: The mesh of L3 vertebra with 5 different bony structures.

The material behaviors of bone structure affect the accuracy of model. Most of studies were modeled the cortical and endplates with same isotropic elastic material behavior. Table 4.1 illustrates the material properties of cortical bone at several studies. Most of studies use isotropic elastic material to model the cancellous bone. However, some recent studies use anisotropic elastic model because the mechanical behavior of cancellous bone is similar to cellular solids, such as polymeric foam [82]. Table 4.2 illustrates the material properties of cancellous bone at several studies. The posterior bone was also modeled with isotropic elastic

material, but lower elastic modulus. The Young's modulus for posterior is usually 3500 MPa with Poisson's ratio 0.25~0.3. Table 4.3 illustrates the material properties of posterior bone at several studies.

Table 4.1: The material properties of cortical bone at several studies

		Cortical Bone			
Study	**Level**	**Elastic Modulus(MPA)**	**Poisson's Ratio**	**Element**	**Transverse Isotropic**
Pitzen [80]	L3-L4	12,000	0.3	S4	-
Natarajan[77]	L3-L5	12,000	0.3	C3D20	-
Rohlmann [56]	L1-L5	10,000	0.3	C3D8	-
Polikeit [83]	L2-L3	12,000	0.3	C3D8	-
Tian-Xia [81]	T10-T11	10,000	0.3	C3D8	-
Guilhem [79]	L2-L4	12,000	0.3	C3D8R	-
Gwanseob [84]	L1-L5	12,000	0.3	C3D8	-
Sairyo [85]	L3-L5	12,000	0.3	C3D8	-

Table 4.2: The material properties of cancellous bone at several studies

		Cancellous Bone			
Study	**Level**	**Elastic Modulus(MPA)**	**Poisson's Ratio**	**Element**	**Transverse Isotropic**
Pitzen [80]	L3-L4	25	0.2	C3D8	Isotropic
Natarajan [77]	L3-L5	100	0.2	C3D20	Isotropic
Rohlmann [56]	L1-L5	200/140	0.45/0.315	C3D8	Transverse
Polikeit [83]	L2-L3	100	0.2	C3D8	Isotropic
Tian-Xia [81]	T10-T11	100	0.2	C3D8	Isotropic
Guilhem [79]	L2-L4	100	0.2	C3D8R	Isotropic
Gwanseob [84]	L1-L5	100	0.2	C3D8	Isotropic
Sairyo [85]	L3-L5	100	0.2	C3D8	Isotropic

Table 4.3: The material properties of posterior bone at several studies

		Posterior Bone			
Study	**Level**	**Elastic Modulus(MPA)**	**Poisson's Ratio**	**Element**	**Transverse Isotropic**
Pitzen [80]	L3-L4	3,500	0.25	C3D8	Isotropic
Natarajan [77]	L3-L5	3,500	0.25	C3D20	Isotropic
Rohlmann [56]	L1-L5	3,500	0.25	C3D8	Transverse
Polikeit [83]	L2-L3	3,500	0.25	C3D8	Isotropic
Tian-Xia [81]	T10-T11	3,500	0.25	C3D8	Isotropic
Guilhem [79]	L2-L4	3,000	0.3	C3D8R	Isotropic
Gwanseob [84]	L1-L5	7,000	0.25	C3D8	Isotropic
Sairyo [85]	L3-L5	3,500	0.25	C3D8	Isotropic

The material properties and element types of bony structures in this study are summarized in Table 4.4.

Table 4.4: The material properties and element types of bony structure in this study

Bony Structure	**Elastic Modulus(MPA)**	**Poisson's Ratio**	**Element**	**Transverse Isotropic**
Cortical Bone	12,000	0.3	C3D4	Isotropic
Cancellous Bone	100	0.2	C3D4	Isotropic
Posterior Bone	3,500	0.35	C3D4	Isotropic
Upper Endplate	12,000	0.3	C3D4	Isotropic
Lower Endplate	12,000	0.3	C3D4	Isotropic

4.5. Intervertebral Disc

The geometry of the annulus fibrosus and nucleus pulposus were created in Mimics and exported to Hypermesh with STL format. The nucleus pulposus covers approximately 45% of the cross sectional area of whole IVD. In Hypermesh, the annulus fibrosus was meshed with hexahedral elements, whereas the nucleus pulposus was meshed with tetrahedral elements. Finally 8 layers of fibers were created with truss elements. The nucleus pulposus was meshed with tetrahedral elements (C3D4). The annulus fibrosus was modeled with hexahedral elements (C3D8), while annulus fibers were modeled with truss elements (T3D2).

The material of intervertebral disc has crucial effect in results of ROM and load sharing. All studies treat the material of the nucleus pulposus as the fluid like material. Most studies model the nucleus pulposus with the Poisson's ratio approximately 0.5 and small elastic modulus. Some studies use fluid elements with bulk modulus to model nucleus pulposus. A comparison of the material property of the nucleus pulposus used in different publications is shown in Table 4.5.

Most studies assume the annulus fibrosus ground substance as a rubber like solid. It is modeled with small elastic modulus. The annulus composite behavior is simulated with truss elements attached to annulus ground. Other ways to model annulus fibers are using shell elements or solid elements with composite properties. In the study, annulus fibers cover approximately 20% of the cross sectional area of the annulus fibrosus and the strength of fibers decrease from outermost layer to innermost layer. A comparison of the material properties of the annulus ground substance and annulus fibers used in different publications are shown in Table 4.6 and Table 4.7, respectively.

Table 4.5: The material properties of nucleus pulposus at several studies

		Nucleus Pulposus			
Study	**Level**	**Elastic Modulus(MPA)**	**Poisson's Ratio**	**Element**	**Transverse Isotropic**
Pitzen [80]	L3-L4	1	0.4999	C3D8	Isotropic
Natarajan [77]	L3-L5	0.2	0.4999	C3D20	Isotropic
Rohlmann [56]	L1-L5	Incompressible	Fluid	F3D4	-
Polikeit [83]	L2-L3	0.2	0.499	C3D8H	Isotropic
Tian-Xia [81]	T10-T11	1	0.499	C3D8	Isotropic
Guilhem [79]	L2-L4	0.1	0.499	C3D8R	Isotropic
Gwanseob [84]	L1-L5	1	0.499	C3D8	Isotropic
Sairyo [85]	L3-L5	1	0.499	C3D8	Isotropic

Table 4.6: The material properties of annulus ground substance at several studies

		Annulus Ground Substance			
Study	**Level**	**Elastic Modulus(MPA)**	**Poisson's Ratio**	**Element**	**Transverse Isotropic**
Pitzen [80]	L3-L4	4.2	0.45	C3D8	Isotropic
Natarajan [77]	L3-L5	4.2	0.45	C3D20	Isotropic
Rohlmann [56]	L1-L5	C_{10}=0.3448 D_1=0.3	-	C3D8H	Neo-Hookean
Polikeit [83]	L2-L3	4.2	0.45	C3D8	Isotropic
Tian-Xia [81]	T10-T11	4.2	0.45	C3D8	Isotropic
Guilhem [79]	L2-L4	4.2	0.45	C3D8R	Isotropic
Gwanseob [84]	L1-L5	4.2	0.45	C3D8	Isotropic
Sairyo [85]	L3-L5	4.2	0.45	C3D8	Isotropic

Table 4.7: The material properties of annulus fibers at several studies

		Annulus Fibers			
Study	**Level**	**Elastic Modulus(MPA)**	**Poisson's Ratio**	**Element**	**Layers**
Pitzen [80]	L3-L4	450	0.3	T3D2	3
Natarajan [77]	L3-L5	Nonlinear		T3D2	5
Rohlmann [56]	L1-L5	Nonlinear	-	Spring	7
Polikeit [83]	L2-L3	360-550	0.3	T3D2	6
Tian-Xia [81]	T10-T11	500	0.3	C3D8	4
Guilhem [79]	L2-L4	360-550	0.3	T3D2	4
Gwanseob [84]	L1-L5	450	0.3	S4	3
Sairyo [85]	L3-L5	Composite	-	C3D8	7

The material properties and element types of IVD structure in this study are summarized in Table 4.8.

Table 4.8: The material properties and element types of IVD structure in this study

IVD Structure	Elastic Modulus(MPA)	Poisson's Ratio	Element	Area(mm^2)
Nucleus Pulposus	1	0.499	C3D4	-
Annulus Ground	4.2	0.45	C3D8	-
Fiber layer 1&2(outermost)	550	0.3	T3D2	0.5
Fiber layer 3&4	495	0.3	T3D2	0.39
Fiber layer 5&6	413	0.3	T3D2	0.31
Fiber layer 7&8(innermost)	360	0.3	T3D2	0.29

4.6. The Facet Joints

Modeling of facets is very crucial as they control the motion of the spine. In this study, the facet joints were simulated with three-dimensional gap contact elements (GAPUNI). These elements transfer force along a single direction as a specified gap closes between nodes. Each facet joint was simulated using 31 gap elements. Initial gap of 2.0 mm was defined between the inferior and superior facets based on the CT images.

The behavior of facet was simulated with ABAQUS's "softened contact" parameter which adjusts force transfer between nodes exponentially, depending on the gap size. The joint assumed the same stiffness as the surrounding bone at full closure. This soft contact and GAP elements could greatly improve the analysis time and decrease the numerical divergence. The soft contact follows the exponential pressure-overclosure relationship given in the following equation with c = 0.1mm and p_0= 0.3 MPa.

$$p = 0 \qquad h < -c$$
$$p = \frac{p_0}{e-1}\left[\frac{1}{c}\left(\frac{h}{c}+2\right)exp\left(\frac{h}{c}+1\right)-\frac{1}{c}\right] \qquad h > -c \qquad \textbf{Eq. 4.1}$$

p: $Pressure$
h: $Overclosure$
c: $Overclosure\ when\ p = 0$
p_0: $Pressure\ when\ h = 0$

4.7. The Spinal Ligaments

Several studies have used linear elastic tension only material model to simulate the spinal ligaments. However, the ligaments exhibit a non linear behavior as shown in Figure 2.9. This approximation cause significant error in the results of analysis. Therefore, most studies adopt a bilinear elastic tension only material model [18-19]. Each linear segment corresponds to the neutral zone and elastic zone. Besides, some recent studies adopt a nonlinear hyper elastic material. Although hyper elastic material models work perfectly in ligament nonlinear complex behavior, they cannot be tension only property.

In this study, firstly truss elements with bilinear elastic tension only material were used to model ligament. A subroutine was written to provide bi-linearity in elastic zone. However, due to unexpected errors in subroutine execution, the 3D axial connector elements with custom bilinear elastic behavior were used in this study. Bi-linearity is created by inputting three points of the experimental load displacement data. Nevertheless, using axial connector has its own inconvenient aspect. In the literature, small strain Young's modulus, transition strain, large strain Young's modulus, and cross sectional area of every ligament are defined [18-19]. However, axial connector takes load displacement data as input. Three load and displacement values should be calculated for every element that represent ligament in the model. This procedure might cost lot of time. Instead of that, average distance was calculated for every ligament type. Three load and displacement values were calculated for every ligament type. Table 4.9 summarizes the ligaments' properties. Figure 4.9 illustrates the position of ligaments in the model.

Table 4.9: Summary of the ligament's properties

Ligament	ALL	PLL	LF	ITL	CL	ISL	SSL
Small strain Young's modulus (Mpa)	7.8	10	15	10	7.5	10	8
Transition strain	12	11	6.2	18	25	14	20
Large strain Young's modulus (Mpa)	20	20	19	59	33	12	15
Cross sectional area	63.7	20	40	1.8	30	40	30
Average length (mm)	12.5	8	19	28.5	3.5	8	22.5
Number of elements	7	4	4	2	4	5	2

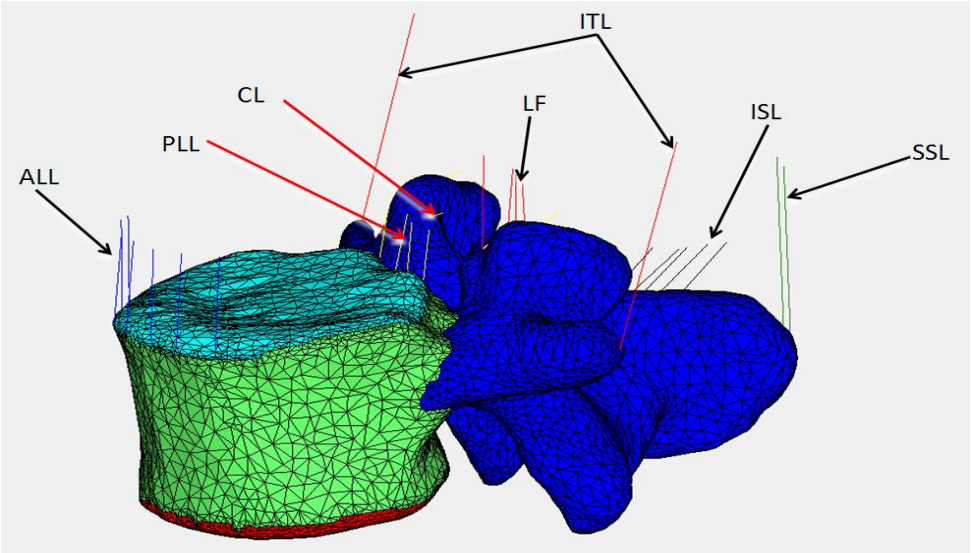

Figure 4.9 : The position of spinal ligaments in the model

4.8. The Summary of L3-L4 Segment Model

Figure 4.10 illustrates the final finite element model of L3-L4 segment.

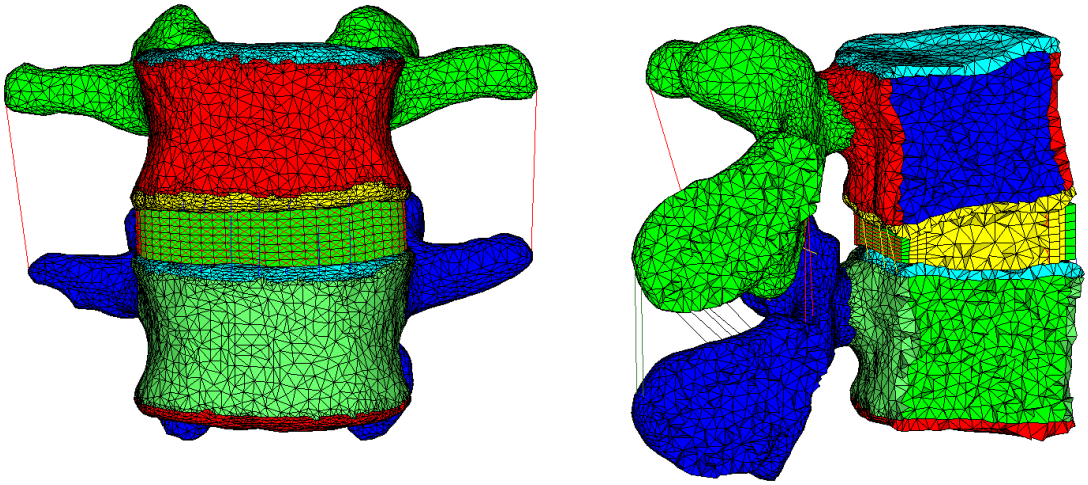

Figure 4.10 : The final finite element model of L3-L4 segment.

Element types and the material properties of all components for the L3-L4 segment model are listed in Table 4.10.

Table 4.10: Element types and the material properties for the L3-L4 segment model

Parts	Elastic Modulus (MPa)	Poisson's Ratio	Area (mm^2)	Element Type	# of Element
Cortical Bone	12,000	0.3	-	C3D4	26535
Cannellous Bone	100	0.2	-	C3D4	43206
Posterior Bone	3,500	0.35	-	C3D4	54595
Endplate Bone	12,000	0.3	-	C3D4	19024
Nucleus Pulposus	1	0.4999	-	C3D4	3872
Annulus Ground	4	0.45	-	C3D8	1176
Annulus Fiber 1&2	550	0.3	0.5	T3D2	784
Annulus Fiber 3&4	495	0.3	0.39	T3D2	784
Annulus Fiber 5&6	413	0.3	0.31	T3D2	784
Annulus Fiber 7&8	360	0.3	0.29	T3D2	784
Facet Joints	Softened		20	GAPUNI	62
Ligaments	**Force(N)-Disp(mm)**		**Area (mm^2)**	**Element Type**	**# of Element**
ALL	0.0 - 0.0 8.52 - 1.5 168.68 - 12.5		63.7	CONN3D2	7
PLL	0.0 - 0.0 5.5 - 0.88 94.5 - 8.0		20	CONN3D2	4
LF	0.0 - 0.0 9.3 - 1.178 187.52 - 19.0		40	CONN3D2	4
ITL	0.0 - 0.0 1.62 - 5.13 45.16 - 28.5		1.8	CONN3D2	2
CL	0.0 - 0.0 14.1 - 0.875 199.73 - 3.5		30	CONN3D2	8
ISL	0.0 - 0.0 11.2 - 1.12 93.76 - 8.0		40	CONN3D2	5
SSL	0.0 - 0.0 24.0 - 4.5 204.0 - 22.5		30	CONN3D2	2

4.9. Implementation of Screws and Implants to the L3-L4 Segment Model

The 3D solid drawings of the screws and implants were created in Unigraphics, and exported to Mimics in the STL format. In mimics, screws and

implants are carefully inserted to L3 and L4 vertebrae to simulate post operative condition. After new positions were determined, the screws and implants were exported to Hypermesh in the STL format. In Hypermesh, the screws and implants were meshed with C3D4 tetrahedral elements. Surfaces between the screws and vertebra bodies were created with morphing operations in Hypermesh.

Two types of screws and two types of implant were used in the study. First type of screw is traditional rigid pedicle screw. It does not allow motion between the screw head and the threaded portion of the screw. Second type is polyaxial pedicle screw. It has a hinge joint simulated between the screw head and the threaded portion of the screw, as illustrated in Figure 4.11. The hinge joint was modeled as a revolute joint between the screw and the hinge. The poly axial pedicle screw allows 17.5° rotation along the hinge. In the model, a 17.5° constraint was defined by the frictionless contact between the nodes of the hinge boundary and the surfaces of the screw. Some of the rotation ability of the screw is lost during implementation to vertebra due to anatomic curve. Both types of screw are 6.00 mm diameter and 55 mm in length. Also, the implementation was bilateral. Surfaces were created between the screws and vertebra bodies. The interaction between the screw shaft and bone, screw head and rod were simulated using the 'tie' constraint. The 'tie' constraint forces nodes that there is no relative motion between them. The threads in both types of screws were ignored because screw bone interface is not an issue of this study. First type of implant is rigid rod system which has 6.0 mm diameter and 50 mm length. Other type is dynamic implant whose development procedure was explained in Chapter 2. The implants and screws are made of Ti_6Al_4V with 115 GPa elastic modulus and 0.36 poison's ratio. Yield and ultimate stresses of Ti_6Al_4V are 1030 MPa and 1150 MPa, respectively.

In this system, intact L3-L4 model and four types of screw-implant systems were investigated. These systems were rigid screw-rigid rod system, rigid screw-dynamic implant system, polyaxial screw-rigid rod system, and polyaxial screw-dynamic implant system. Figure 4.12 illustrates implemented rigid screw-rigid rod system and polyaxial screw-dynamic implant system.

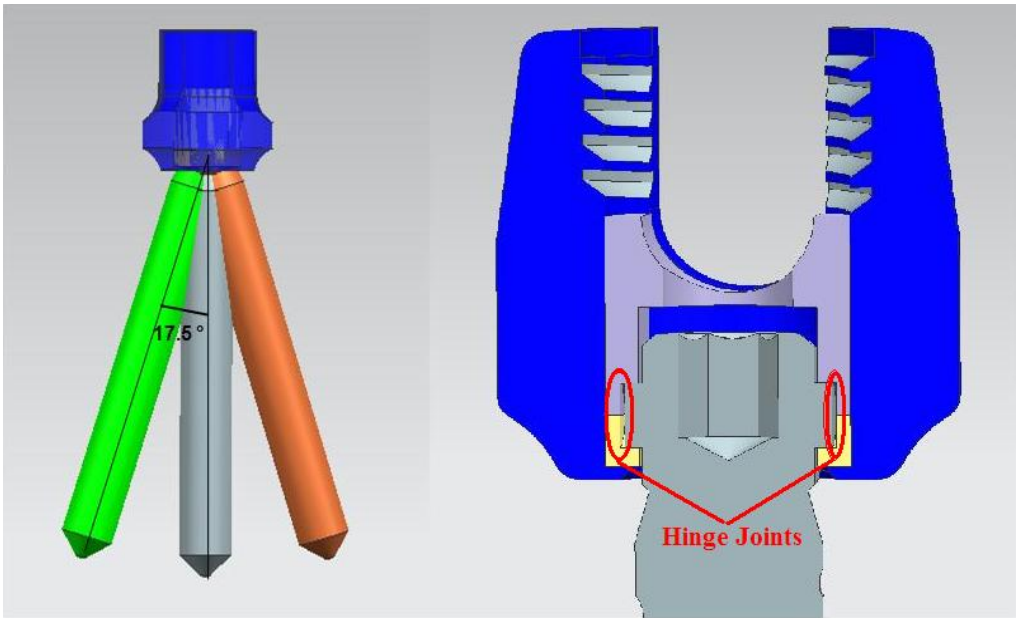

Figure 4.11: The poly axial pedicle screws

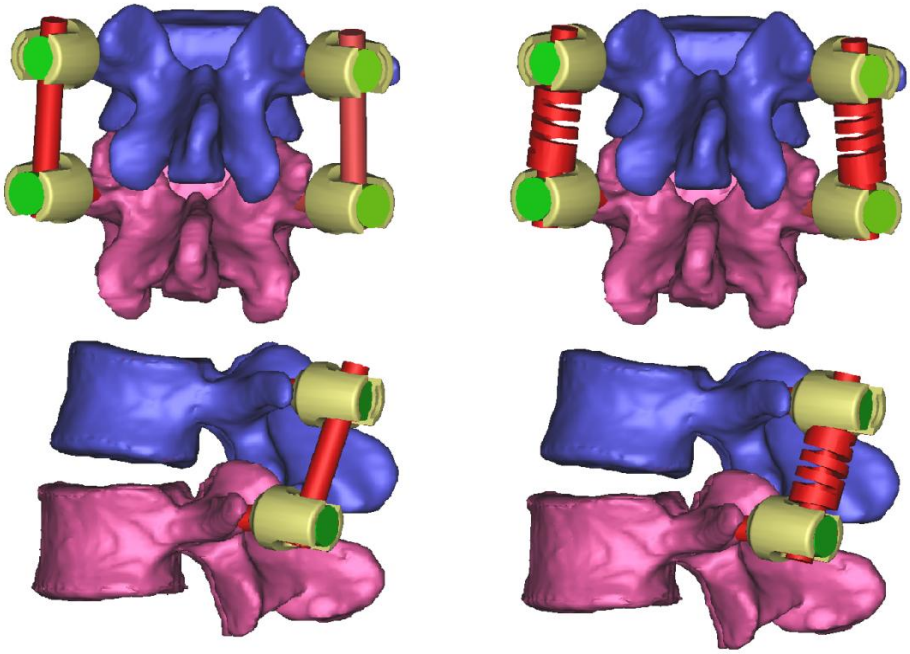

Figure 4.12: Implemented rigid screw-rigid rod system and polyaxial screw-dynamic implant system

4.10. Boundary Conditions and Loadings

The inferior surface of L4 endplate was constrained in all the six degrees of freedom. A preload of 400N was applied on the superior surface of L3 endplate to simulate body weight. The compressive load was applied on the superior surface of L3 endplate as an evenly distributed load. A bending moment was applied on the superior surface of L3 endplate to simulate physiological motions including flexion, extension, lateral bending, and axial rotation. The finite element model of L3-L4 segment is almost symmetric about the mid sagittal plane. Due to symmetry, only the right rotation and right bending were computed.

Flexion, extension, lateral bending, and axial rotation motions were investigated with a load control protocol. This protocol includes an axial compressive force of 400 N which represent body weight, and a moment. In all motions, moment was applied up to 10.0 Nm, in steps of 1.0 Nm. The load control protocol was employed for intact L3-L4 segment model and all four screw-implant systems. The segmental ranges of motion for all cases were examined by the load control protocol. Another criterion in evaluation of new implant is load sharing characteristic. The amount of load shared by the intervertebral disc, facet joints, and the various posterior stabilization systems was computed. An axial compressive load of 400N was simulated, which would be distributed between the disc and the posterior stabilization system. Load sharing will be quantified for both intact without instrumentation and the intact with instrumentation models. Figure 4.13 shows the boundary and loading surfaces.

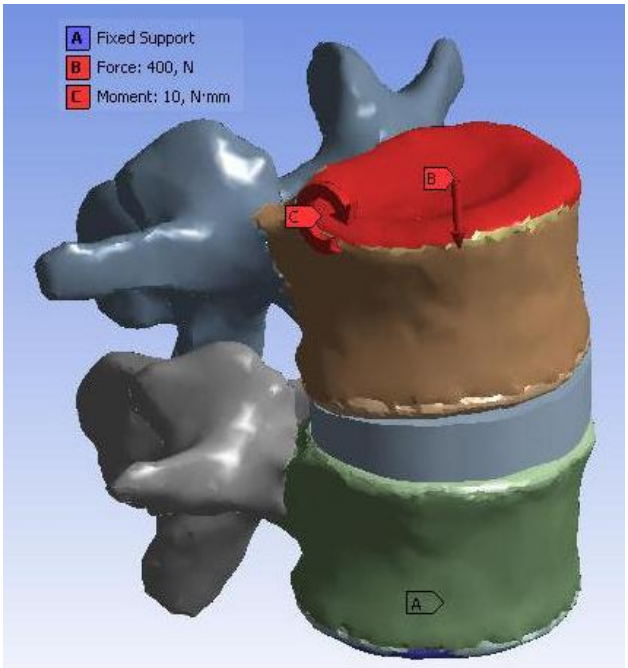

Figure 4.13: The boundary and loading surfaces

4.11. Data Analysis

Rotation motion characterizes the segmental stability. The rotational angles were calculated using the nodal deformation of a constant a set of nodes, because relative rotational angle calculation is not supported by ABAQUS. A Python script was written to read ABAQUS result file and calculate relative rotation angle directly.

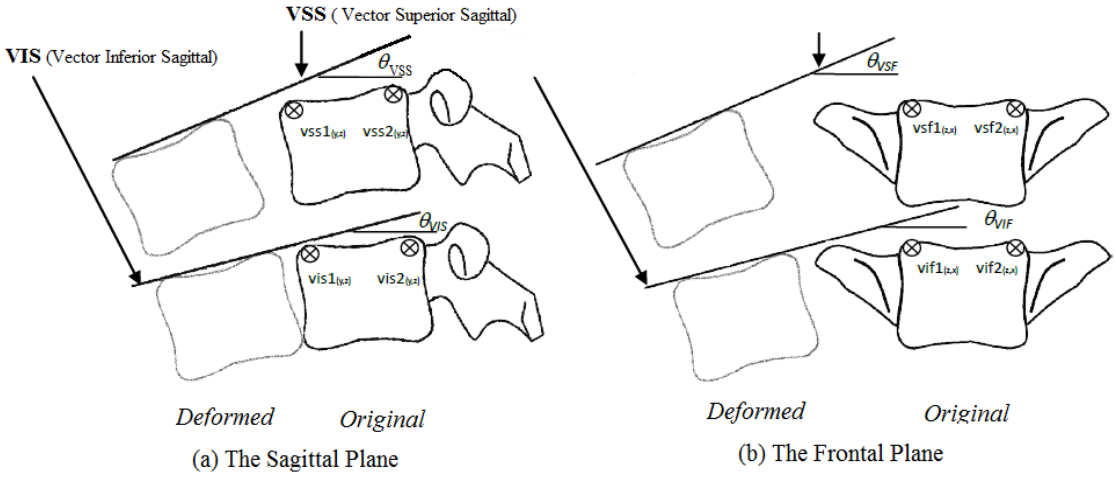

Figure 4.14: The definition of displacement direction of a FSU ($\theta_2 - \theta_1$ is the relative rotational angle of an adjacent vertebra)

The Figure 4.14 defines four space vectors, VSS (Vector Superior Sagittal), VIS (Vector Inferior Sagittal), VSF (Vector Superior Frontal), and VIF (Vector Inferior Frontal). Each sagittal vector was defined by two points within one plane coordinate, ex: $VSS_{(y,z,t)} = vss2_{(y,z,t)} - vss1_{(y,z,t)}$, and the definitions of rest of $VIS, VSF, and\ VIF$ are similarly visualized in Figure 4.14. For an example, the sagittal (yz) plane relative rotational angle $\theta_{yz}(t)$ equals the difference between absolute coordinate angle $\theta_{VSS}(t)$ and $\theta_{VIS}(t)$ from Equation 4.2.

$$\theta_{VEC}(t) = tan^{-1}\left(\frac{VEC_{[z](t)}}{VEC_{[y](t)}}\right) \qquad \boldsymbol{Eq.4.2}$$

$Where$:
$\theta_{VEC}(t) : Absolute\ coordinate\ angle\ of\ particular\ spatial\ vector\ at\ time, t$
$VEC_{[z]} : z\ component\ value\ of\ particular\ spatial\ vector\ at\ time, t$
$VEC_{[y]} : y\ component\ value\ of\ particular\ spatial\ vector\ at\ time, t$

Chapter 5 : Model Validation and Results

5.1. Model Validation

The finite element model of intact L3-L4 was validated for further analysis by comparing model predictions of load displacement behavior with values reported in the literature.

In Schultz et al. study, mechanical behavior of 42 cadaver lumbar motion segments were obtained under flexion, extension, lateral bending, and axial rotation. Schultz et al. reported the load displacement properties in all principal directions with a compressive preload of 400N [86]. This preload of 400 N was maintained while moments (4.7Nm and 10.6 Nm) about the three principal axes were applied individually. Average motion results were reported from 11 L1-L2 segments, 8 L2-L3 segment, 13 L3-L4 segments, and 10 L4-L5 segments. Table 5.1 provides a comparison of the model predictions in flexion, extension, lateral bending, and axial rotation with those reported by Schultz et al. L3-L4 model was validated because FE model prediction fall within one standard deviation of Schultz et al. results [86]. Although axial rotations are overestimated, flexion is very close to in vitro results for first and second loading cases. Error in lateral bending and rotation results for high loading case is small, but error is bigger in lateral bending and rotation results for low loading case.

Table 5.1: Comparison of L3-L4 model prediction and Schultz et al.[86] results

4.7 Nm moment + 400 N compression	**L3-L4 model prediction**	**Schultz et al. Results**
Flexion	4.4°	5.13 ± 1.86°
Extension	2.6°	2.12 ± 0.98°
Right Lateral Bending	2.9°	4.47 ± 1.63°
Right Axial Rotation	1.1°	0.69 ± 0.33°
10.6 Nm moment + 400 N compression		
Flexion	5.4°	5.51 ± 1.00°
Extension	3.2°	2.99 ± 1.02°
Right Lateral Bending	5.4°	5.64 ± 1.22°
Right Axial Rotation	1.9°	1.5 ± 0.67°

5.2. Results

Posterior dynamic stabilization implants are widely used to reduce loading of the intervertebral disc and facet joints for treatment of chronic lower back pain while preserving the motion within normal physiological limits. Pain is removed by unloading pressure on it. Adjacent segment disease can be prevented if range of motion of implemented segment is similar to intact segment. Therefore, load sharing characteristic of implant and effect of implant to segmental range of motion are two main criteria in evaluation of the newly developed implant. Effect of implant to segmental range of motion and load sharing characteristic of implant were investigated in the analysis.

Flexion, extension, lateral bending, and axial rotation motions were investigated with a load control protocol. This protocol includes an axial compressive force of 400 N which represent body weight, and a moment. In all motions, moment was applied up to 10.0 Nm, in steps of 1.0 Nm. The load control protocol was employed for intact L3-L4 segment model and all four screw-implant systems. These systems were rigid screw-rigid rod system, rigid screw-dynamic implant system, polyaxial screw-rigid rod system, and polyaxial screw-dynamic

implant system. The effects of the systems to segmental ranges of motion for all cases were examined by the load control protocol.

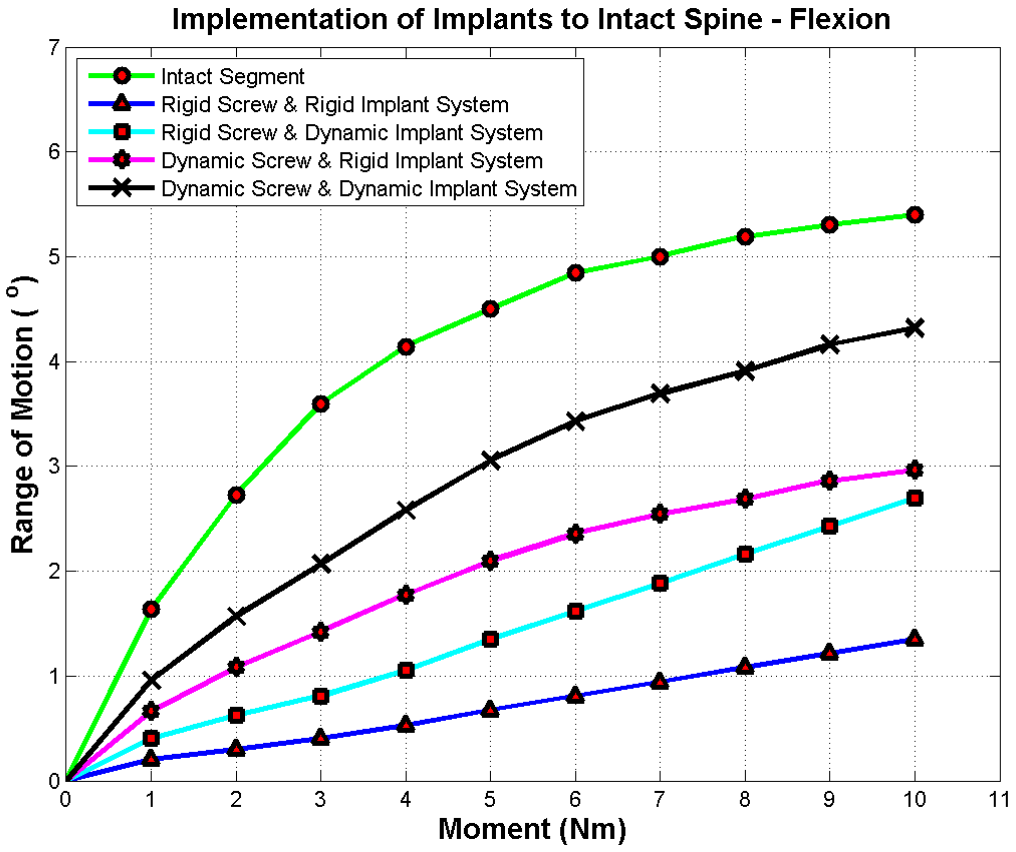

Figure 5.1: Range of motion in flexion

The segmental range of motion in flexion with respect to the intact from the simulations of rigid screw-rigid rod system, rigid screw-dynamic implant system, polyaxial screw-rigid rod system, and polyaxial screw-dynamic implant system were evaluated, as shown in Figure 5.1. Trend of predicted motion for intact segment perfectly fits physiological curve of healthy spine. Stiffness of intact spine increases as the loading is increasing due to nonlinearity of ligament and facet joints behavior. At the beginning of loading, L3 vertebra rotates approximately 1° in flexion at 1Nm loading. This relatively big rotation is caused from low stiffness value of ligament and low reaction force in facet joints. As explained in Chapter 4.7, the spinal ligaments were modeled with bilinear material model. At the small strain, the stiffness of ligament is low. As the strain increases, the stiffness value of ligaments passes second linear region in which stiffness is higher. At higher loading case, the

stiffness of intact segment increases rapidly. This is caused by facet contact behavior. As explained in Chapter 4.6, the facet transfer forces between nodes exponentially, depending on the gap size. The contact follows the exponential pressure-overclosure relationship. Therefore, as gap closes at higher loading, the reaction forces at the facet increases exponentially.

In flexion, the rigid screw-rigid implant system greatly reduces the motion by 75%. Stiffness of implanted segment is almost constant, because the rigid screw-rigid implant system has dominant role in the segment motion. The segment with the rigid screw-dynamic implant system has almost constant but lower stiffness value. The rigid screw-dynamic implant system reduces the motion by 50%. The segment with the polyaxial screw-rigid implant system has similar motion-moment curve with intact segment. The stiffness of implanted segment increases as the loading raises. However, the polyaxial screw and rigid implant system reduces the motion up to 45%. The segment with the polyaxial screw and dynamic implant system has closer range of motion-moment curve with intact segment relative to other systems. The polyaxial screw and dynamic implant system reduces the motion by 20%. Therefore, last system is superior in flexion.

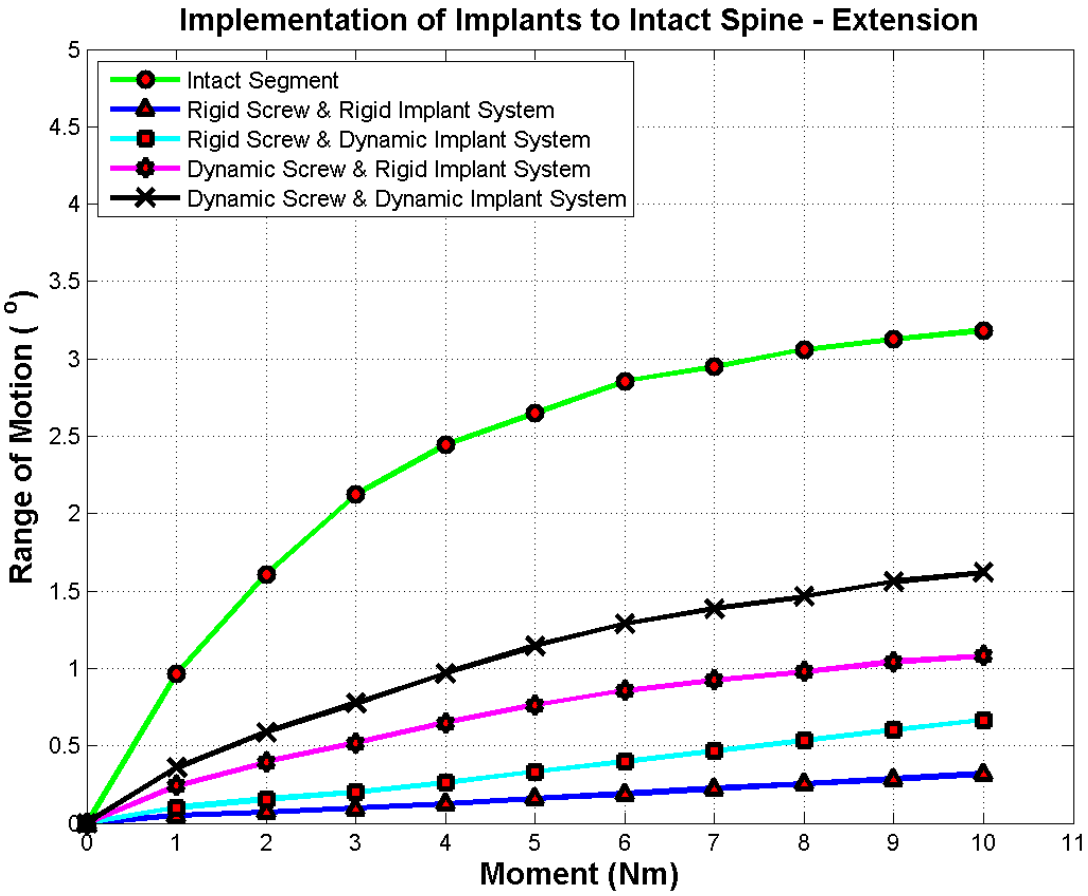

Figure 5.2: Range of motion in extension

In extension, trend of predicted motion for intact segment resembles physiological curve of healthy spine. Stiffness of intact spine increases as the loading is increasing due to nonlinearity of ligament and facet joints behavior. In flexion, the rigid screw-rigid implant system limits the motion by 90%. The rigid screw-rigid implant system determines constant stiffness of segment motion. The segment with the rigid screw-dynamic implant system has almost constant but lower stiffness value. The rigid screw-dynamic implant system reduces the motion up to 79%. The segment with the polyaxial screw-rigid implant system has nonlinear motion-moment curve. The stiffness of implanted segment slightly increases as the loading raises. This increase is not significant as in flexion. The polyaxial screw-rigid implant system reduces the motion by 66.08%. The polyaxial screw-dynamic implant system reduces the motion by 49.12%.

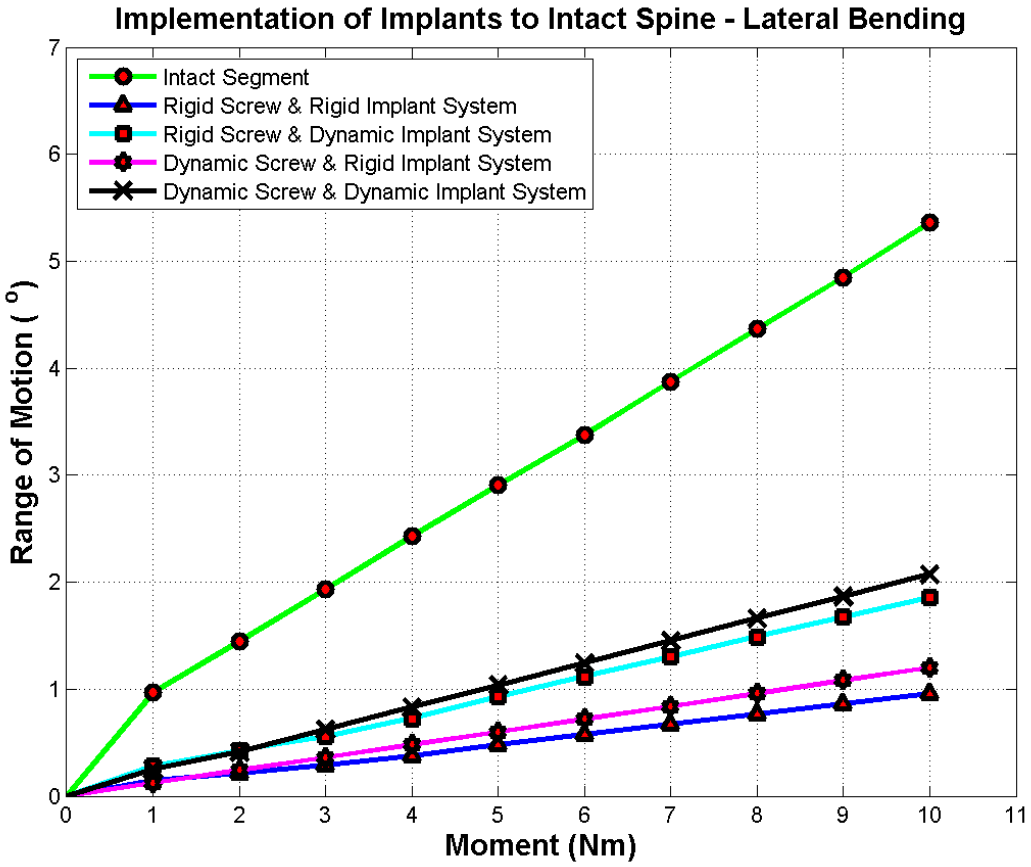

Figure 5.3: Range of motion in lateral bending

In lateral bending, there is a difference between predicted motion curve of intact segment and physiological curve of healthy spine, but overall prediction of motion fall within one standard deviation of Schultz et al. [86] results at least two loading points. Stiffness of intact spine is constant. In lateral bending, the rigid screw-rigid implant system limits the motion up to 82.18%. Unlike flexion and extension, in lateral bending, the polyaxial screw-rigid screw system has constant but lower stiffness value. In flexion and extension, the polyaxial screw-rigid screw system has a nonlinear motion moment curve that resembles physiological curve of healthy spine. The polyaxial screw-rigid screw system show similar behavior with the rigid screw-rigid implant system in lateral bending, because the hinge joint allows rotation in flexion and rotation, but limits rotation in lateral bending. The polyaxial screw-rigid implant system reduces the motion by 77.62%. The rigid screw-dynamic implant system creates less stiff system in lateral bending. The rigid

screw-dynamic implant system reduced the motion by 65.35%. The polyaxial screw and dynamic implant system resembles the rigid screw-dynamic implant system, and reduces the motion up to 61.34%.

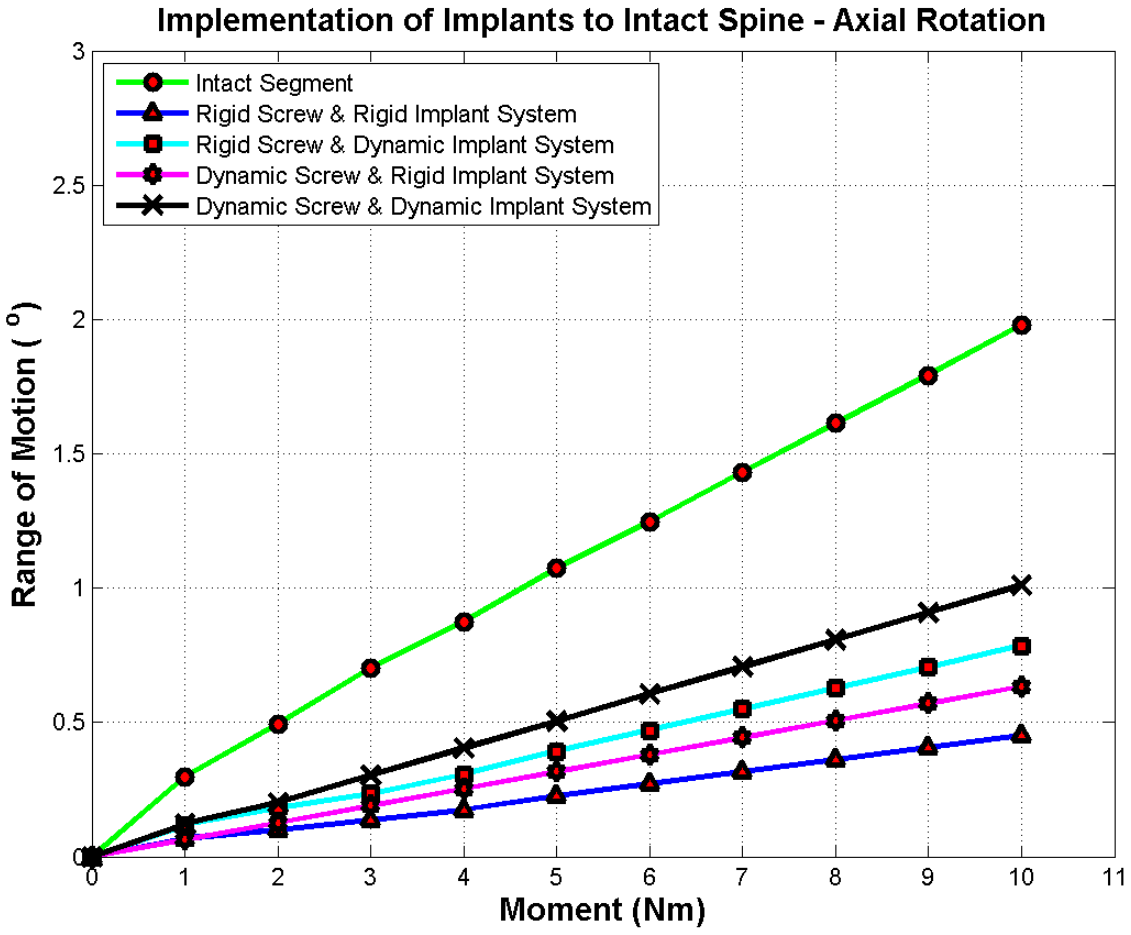

Figure 5.4: Range of motion in axial rotation

In axial rotation, a difference was occurred between predicted motion curve of intact segment and physiological curve of healthy spine. Stiffness of intact spine is almost constant. In axial rotation, the rigid screw-rigid implant system limits the motion by 77.23%. In axial rotation, the polyaxial screw-rigid screw system has constant but lower stiffness value, similar to lateral bending case. The polyaxial screw-rigid screw system behaves similar to the rigid screw-rigid implant system in axial rotation, because the hinge joint allows rotation in flexion and rotation, but limits rotation in axial rotation. The polyaxial screw-rigid implant system reduces the motion by 68% in axial rotation. The rigid screw-dynamic implant system creates less stiff system in axial rotation. The rigid screw-dynamic implant system reduced

the motion up to 60.4%. The polyaxial screw-dynamic implant system gives relatively good results. The system reduces the axial rotation by 49%.

Table 5.2 presents the summary of angular displacement and the percentage changes compared to the intact case of models in 400N compression and 10.0 Nm moments.

Table 5.2: The summary of angular displacement under 400N compression and 10Nm moment.

400N + 10Nm	Flexion		Extension	
	Prediction	**Change (%)**	**Prediction**	**Change (%)**
Intact segment	5.4	-	3.2	-
Rigid screw &Rigid Implant	1.3	-75	0.3	-90
Rigid screw &Dynamic Implant	2.7	-50	0.7	-79
Polyaxial screw &Rigid Implant	3.0	-45	1.1	-66
Ployaxial screw &Dynamic Implant	4.3	-20	1.7	-49
	Lateral Bending		**Axial Rotation**	
	Prediction	**Change (%)**	**Prediction**	**Change (%)**
Intact segment	5.4	-	2.0	-
Rigid screw &Rigid Implant	1.0	-82	0.5	-77
Rigid screw &Dynamic Implant	1.9	-65	0.8	-60
Polyaxial screw &Rigid Implant	1.2	-78	0.6	-68
Ployaxial screw &Dynamic Implant	2.1	-61	1.0	-49

In addition to effect of implant to segmental range of motion, load sharing characteristic of implant is important criteria in evaluation of implant. The implant must share load to remove the pressure on the nerve. The amount of load shared by the intervertebral disc, facet joints, and the various posterior stabilization systems was computed. An axial compressive load of 400N was simulated, which would be distributed between the disc and the posterior stabilization system. Load sharing will be quantified for both intact without instrumentation and the intact with instrumentation models.

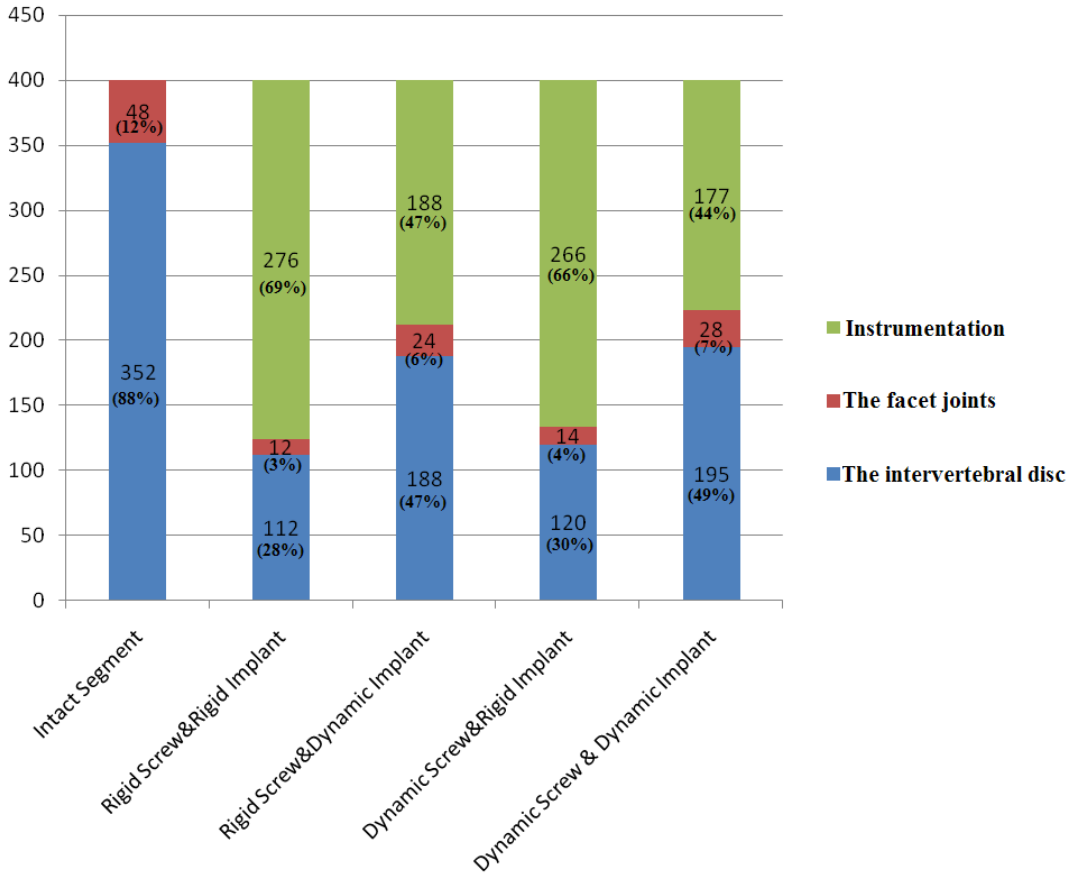

Figure 5.5: Load sharing characteristic of intact segment and four systems

The intact model showed that 12% of the compressive load (48N) is shared by the facet joints. All fixation systems reduce the facet and intervertebral disc load. The facet load for the rigid screw-rigid implant system decreased up to 12N (25% of intact case). The rigid screw-rigid implant system and the polyaxial screw-rigid implant system have similar loads sharing characteristic. Likely, the rigid screw-dynamic implant system and the polyaxial screw-dynamic implant system have similar load sharing. Dynamic implant improves load sharing capacity of system.

To sum up, the rigid screw-rigid implant system greatly reduces the motion in all loading. This fixation system transmits compressive load through itself instead of sharing load with the facet joints and intervertebral disc. The rigid screw-dynamic implant system reduces the motion by 50% in flexion, 79% in extension, 66.35% in lateral bending, and by 60.4% in axial rotation. The reduction of motion for the rigid screw-dynamic implant system is significantly less than the rigid screw and rigid

implant system. Besides, using dynamic implant instead of rigid one improves the load sharing. The polyaxial screw-rigid implant system reduces the motion by 45% in flexion, by 66.08% in extension, by 77.35% in lateral bending, and by 68% in axial rotation. The trend of segment motion in flexion and extension is in agreement with trend of physiological motion of healthy segment. However, in lateral bending and axial rotation, the polyaxial screw shows similar behavior with rigid screw because the hinge link allows motion in flexion and extension, but limits motion in lateral bending and axial rotation. Nevertheless, this system transmits compressive load through itself instead of sharing load with the facet joints and intervertebral disc, similar to rigid screw. The polyaxial screw-dynamic implant system exhibits the best results for segmental range of motion and load sharing characteristics within four stabilization systems. The reduction of motion in all loadings is minimum within four stabilization systems. In addition to that, the trend of segment motion is similar to intact segment motion in flexion and extension. Also, this stabilization system share load with the intervertebral disc and the facet joints.

Chapter 6 : Conclusion & Future Work

6.1. Conclusion

Low back pain is a major health problem worldwide at any age, but especially at an elderly age. Treatment options may vary from conservative treatment to fusion. Fusion is a traditional technique for stabilization. However, while fusion relieves back pain early, pain is likely to return due to facet hypertrophy, facet arthropathy, spinal stenosis, osteophyte formation, and posterior muscular debilitation, as well as disc degeneration at adjacent levels to the fusion site. Therefore, non-fusion techniques are currently being investigated and often used for treatment options.

Posterior dynamic stabilization implants are intended to provide physiological motion at the treated level, and reduce loading of the intervertebral disc and facet joints. Posterior dynamic stabilization is a new concept, and a few implants are currently in the market. In this study, initial implant model was developed that limit abnormal motion at the segment while preserves the motion within normal physiological limits. The effects of design parameters to strength and flexibility of the implant were investigated. Initial design was improved to final design that builds balance between flexibility and strength.

Finite element model of an intact L3-L4 lumbar segment was developed. Load sharing characteristic of implant and effects of implant to segmental range of motion are two main criteria in evaluation of the newly developed implant. Finite element analysis were performed to investigate effects of newly developed implant to the segmental range of motion and load sharing characteristics in lateral bending, flexion, extension, and axial rotation. In this system, intact L3-L4 model and four types of screw-implant systems were investigated. These systems were rigid screw-rigid rod system, rigid screw-dynamic implant system, polyaxial screw-rigid rod system, and polyaxial screw-dynamic implant system.

The polyaxial screw-dynamic implant system exhibits the best results for segmental range of motion and load sharing characteristics within four stabilization systems. The reduction of motion for the polyaxial screw-dynamic implant system in all loading is minimum within four stabilization systems. This stabilization system shares load with the intervertebral disc and the facet joints. The rigid screw-rigid implant system greatly reduces the motion in all loading. The rigid screw-dynamic implant system reduced the motion by 50% in flexion, by 79% in extension, by 66.35% in lateral bending, and by 60.4% in axial rotation. The polyaxial screw-rigid implant system reduces the motion by 45% in flexion, 66.08% in extension, 77.35% in lateral bending, and by 68% in axial rotation. The rigid screw-rigid implant system and the polyaxial screw-rigid implant system have similar loads sharing characteristic. Likely, the rigid screw-dynamic implant system and the polyaxial screw-dynamic implant system have similar load sharing. Dynamic implant improves load sharing capacity of system.

6.2. Future Work

- The current study is restricted to being a finite element analysis, undertaking a cadaveric study would give us more confidence in the model predictions, especially for the poly axial screw and dynamic implant system.
- L3-L4 segment model can be extended to adjacent segments to investigate load sharing characteristic and segmental range of motion of adjacent segment.
- Current finite element model can be improved with inserting spine muscle models into current finite element model.
- Recently the indications for the use of dynamic stabilization have been extended to stabilize an adjacent segment to fusion. A finite element study with dynamic stabilization adjacent to fusion maybe helpful in understanding various biomechanical parameters.

BIBLIOGRAPHY

1. Andersson, G.B., *Epidemiological features of chronic low-back pain.* Lancet, 1999. **354**(9178): p. 581-5.
2. Hart, L.G., R.A. Deyo, and D.C. Cherkin, *Physician office visits for low back pain. Frequency, clinical evaluation, and treatment patterns from a U.S. national survey.* Spine, 1995. **20**(1): p. 11-9.
3. Taylor, V.M., et al., *Low back pain hospitalization. Recent United States trends and regional variations.* Spine, 1994. **19**(11): p. 1207-12.
4. Viscogliosi AG, J.V., MR Viscogliosi, *Beyond total disc, the future of spine surgery.* Spine Industry Analysis Series, 2004.
5. Martin, B.I., et al., *Expenditures and health status among adults with back and neck problems.* JAMA, 2008. **299**(6): p. 656-64.
6. White III A.A., a.P.M.M., *Clinical Biomechanics of the spine*. Second ed. 1990, Philadelphia: Lippincott-Raven.
7. Sheehan JM, C.S., JA Jane, *Degenerative lumbar stenosis: The neurosurgical perspective.* Clin Orthop, 2001. **384**: p. 61-74.
8. Wiltse LL, W.K.-W., GWD McIvor, *The treatment of spinal stenosis.* Clin Orthop, 1976. **115**: p. 83-91.
9. Johnsson KE, S.W., K Johnsson, *Postoperative instability after decompression for lumbar spinal stenosis.* Spine, 1986. **11**(2): p. 107-10.
10. TY., C., *The controversy over diagnosis and treatment of facet pain.* Chin Med Assoc, 2005. **68**(2): p. 51-2.
11. D., B., *Does osteoarthritis of the lumbar spine cause chronic low back pain?* Current Pain and Headache Reports, 2004. **8**: p. 512-7.
12. Vanharanta H, T.F., DD Ohnmeiss, SH Hochschuler, RD Guyer, *The relationship of facet tropism to degenerative disc disease.* Spine, 1993. **18**(8): p. 1000-5.
13. Boden SD, K.R., K Yamaguchi, TP Branch, D Schellinger, SW Wiesel., *Orientation of the lumbar facet joints: association with degenerative disc disease.* Bone Joint Surg, 1996. **78A**(3): p. 403-11.
14. Noren R, J.T., GBJ Andersson, MS Huckman, *The role of facet joint tropism and facet angle in disc degeneration.* Spine, 1991. **16**(5): p. 530-2.
15. Ledet, E.H., et al., *Direct real-time measurement of in vivo forces in the lumbar spine* Spine, 2005. **5**(1): p. 85-94
16. Adams, M.A.a.W.C.H., *The relevance of torsion to the mechanical derangement of the lumbar spine* Spine (Phila Pa 1976), 1981. **6**(3): p. 241-8
17. Korovessis P, e.a., *Rigid, semirigid versus dynamic instrumentation for degenerative lumbar spinal stenosis: a correlative radiological and clinical analysis of short-term results.* Spine (Phila Pa 1976), 2004. **29**: p. 735-742.
18. Dong Suk Shin, K.L., and D. Kim, *Biomechanical study of lumbar spine with dynamic stabilization device using finite element method.* Computer-Aided Design, 2007. **39**(7): p. 559-567.
19. Parepalli, B.K., *Biomechanical Evaluation of Posterior Dynamic Stabilization Systems in Lumbar Spine*, in *College of Engineering* 2009, The University of Toledo Toledo.

20. Deyo, R.A., et al., *United States trends in lumbar fusion surgery for degenerative conditions.* Spine, 2005. **30**(12): p. 1441-5.
21. Denhoy. *Spine Sector Shows Continued Growth, in MX Business Strategies for Medical Technology Executives*. Cannon Communications LLC 2008; Available from: http://devicelink.com/mx/issuesupdate/08/08/Spine.html.
22. Chiang MF, Z.Z., Chen CS, Cheng CK, Shih SL., *Biomechanical comparison of instrumented posterior lumbar interbody fusion with one or two cages by finite element analysis.* Spine., 2006. **31**(19): p. E682-E689.
23. Schmidt H, K.A., Heuer F, Simon U, Claes L, Wilke HJ. , *Intradiscal pressure, shear strain and fiber strain in the intervertebral disc under combined loading Spine* 2007 **32**(7): p. 748-755.
24. Tittel, K., *Beschreibende und funktionelle:Anatomie des Menschen*. 8 ed. 1990: Jena,VEB Gustav-Fischer Verlag.
25. spine, A.o. 2009; Available from: www.spineuniverse.com.
26. Chen, C.-H., *A Finite Element Study of the Biomechanical Behavior of the Nonlinear Ligamentous Thoracic and Lumbar Spine*, in *Department of Civil Engineering*. 2007, National Cheng Kung University.
27. Gregersen G.G., a.L.D.B., *An in vivo study of the axial rotation of the human thoracolumbar spine.* J. Bone Joint Surg., 1967. **49A**: p. 247.
28. Moore L., D.A., *Clinically Oriented Anatomy*. Fifth ed. 2006, Philadelphia: Lippincott Company.
29. Silva M.J., W.J., Keaveny T.M., and Hayes W.C., *Direct and computed tomography thickness measurements of the human,lumbar vertebral shell and endplate.* Bone, 1994. **15**(4): p. 409-414.
30. Nordin M., F.V.H., *Basic biomechanics of the musculoskeletal system*. 2001, Baltimore: Lippincott Williams and Wilkins.
31. Drerup B, G.M., Assheuer J, Zerlett G., *Assessment of disc injury in subjects exposed to long-term whole-body vibration.* Euro Spine J., 1999. **8**(6): p. 458-67.
32. Luoma K, R.H., Raininko R, Luukkonen R, Lamminen A, Viikari-Juntura E., *Lumbar disc degeneration in relation to occupation.* Scand J Work Environ Health, 1998. **24**(5): p. 358-66.
33. Stokes IA, I.J., *Mechanical Conditions That Accelerate Intervertebral Disc Degeneration: Overload Versus Immobilization.* Spine, 2004. **29**(23): p. 2724-32.
34. Ferguson SJ, T.S., *Biomechanics of the aging spine.* Eur Spine J., 2003. **12**(Suppl.2): p. 97-103.
35. Garfin SR, H.H., S Mirkovic, *Spinal stenosis.* Bone Joint Surg, 1999. **81A**(4): p. 572-82.
36. Atlas SJ, K.R., Wu YA, Deyo RA, Singer DE, *Long-term outcomes of surgical and nonsurgical management of lumbar spinal stenosis: 8 to 10 year results from the maine lumbar spine study.* Spine, 2005. **30**(8): p. 936-43.
37. Chen CS, C.C., Liu CL, Lo WH, *Stress analysis of the disc adjacent to interbody fusion in lumbar spine.* Med Eng Phys., 2001. **23**(7): p. 483-91.
38. Rao RD, W.M., Singhal P, McGrady LM, Rao S., *Intradiscal pressure and kinematic behavior of lumbar spine after bilateral laminotomy and laminectomy.* Spine, 2002. **2**(5): p. 320-6.

39. Lee KK, T.E., *Effects of laminectomy and facetectomy on the stability of the lumbar motion segment.* Med Eng Phys., 2004. **26**(3): p. 183-92.
40. Zander T, A.R., C Klockner, G Bergmann, *Influence of graded facetectomy and laminectomy on spinal biomechanics.* Eur Spine 2003 **12**: p. 427-34.
41. Teo EC, L.K., Qiu TX, Ng HW, Yang K., *The biomechanics of lumbar graded facetectomy under anterior-shear load.* IEEE Trans Biomed Eng., 2004. **51**(3): p. 443-9.
42. Turner JA, E.M., Herron L, Haselkorn J, Kent D, Ciol MA, Deyo R., *Patient outcomes after lumbar spinal fusions.* JAMA, 1992. **268**(7): p. 907-11.
43. Van Ooij A, F.O., AJ Verbout, *Complications of artificial disc replacement.* Spinal Disord Techniques, 2003. **16**(4): p. 369-83.
44. Dooris AP, V.G., NM Grosland, LG Gilbertson, DG Wilder, *Load-sharing between anterior and posterior elements in a lumbar motion segment implanted with an artificial disc.* Spine, 2001. **26**(6): p. E 122-9.
45. D.K, S., *Dynamic stabilization devices in the treatment of low back pain.* Orthop Clin North Am., 2004. **35**(1): p. 43-56.
46. Lindsey DP, S.K., Fuchs P, Hsu KY, Zucherman JF, Yerby SA, *The effects of an interspinous implant on the kinematics of the instrumented and adjacent levels in the lumbar spine.* Spine, 2003. **28**(19): p. 2192-7.
47. Bellini, C.M., et al., *Biomechanics of the lumbar spine after dynamic stabilization.* Spinal Disord Techniques, 2007. **20**(6): p. 423-9.
48. Vijay K. Goel, P., Ali Kiapour, MS, Ahmed Faizan, BS, Manoj Krishna, FRCS, MCh(Orth), and Tai Friesem, MD., *Finite Element Study of Matched Paired Posterior Disc Implant and Dynamic Stabilizer (360° Motion Preservation System).* SAS Jounral, 2007. **01**(01).
49. H., G., *Lumbar instability:surgical treatment without fusion.* Rachis 1992. **421**: p. 123-37.
50. Nohara H, K.F., *Biomechanical study of adjacent intervertebral motion after lumbar spinal fusion and flexible stabilization using polyethylene-terephthalate bands.* Spinal Disorders & Techniques 2004. **17**: p. 215-9.
51. Mulholland RC, S.D., *Rationale, principles, and experimental evaluation of the concept of soft stabilization.* Eur Spine, 2002. **11**(2): p. 198-205.
52. Eberlein R, H.G., Schulze-Bauer CAJ., *Assesment of a spinal implant by means of advanced FE modeling of intact human intervertebral discs.* Fifth World congress on computational mechanics. Vienna University of Technology, 2002: p. 1-14.
53. Schmoelz W, H.J., Nydegger T, et al., *Dynamic stabilization of the lumbar spine and its effects on adjacent segments: an vitro experiment.* Spinal Disorders & Techniques, 2003. **16**: p. 418-423.
54. Niosi CA, Z.Q., Wilson DC, keynan O, Wilson DR, Oxland TR. , *Biomechanical characterization of the three dimensional kinematic behaviour of the Dynesys dynamic stabilization system: An vitro study.* European Spine Journal 2006. **15**: p. 913-922.
55. Niosi CA, W.D., Zhu Q, Keynan O, Wilson DR, Ozland TR., *The effect of dynamic posterior stabilization on facet joint contact forces.* Spine, 2008. **33**(1): p. 19-26.

56. Rohlmann, A., et al., *Comparison of the effects of bilateral posterior dynamic and rigid fixation devices on the loads in the lumbar spine: a finite element analysis.* Eur Spine, 2007. **16**(8): p. 1223-31.
57. System, C.; Available from: www.ulrichulm.de/eng/wirbelsaeule/cosmic-intro.html.
58. Zhang QH., T.E., *Finite element application in implant research for treatment of lumbar degenerative disc disease.* Medical Engineering &Physics 2008. **30**: p. 1246-1256.
59. Lau S., L.K., *Lumbar stabilization techniques.* Current Orthopaedics 2007.**21**: p. 25-39.
60. MM., P., *The stabilizing system of the spine. Part II Neutral zone and instability hypothesis.* Journal of Spinal Disorders & Techniques 1992. **5**: p. 390-396.
61. Stokes IA, F.J., *Segmental motion and instability.* Spine, 1987. **12**:p. 688-691.
62. Weiler PJ, K.G., Gertzbein SD., *Analysis of sagittal plane instability of the lumbar spine in vivo.* Spine, 1990. **15**: p. 1300-1306.
63. McNally DS, A.M., *Internal intervertebral disc mechanics as revealed by stress profilometry.* Spine, 1992. **17**: p. 66-73.
64. Boos N, W.J., *Pedicle screw fixation in spinal disorders: a European view.* European Spine Journal 1997. **6**: p. 2-18.
65. Gibson JN, G.I., Waddell G., *The Cochrane review of surgery for lumbar disc prolapse and degenerative lumbar spondylosis.* Spine, 1999. **24**: p. 1820-1832.
66. Weinhoffer SL, G.R., Herbert M, Griffith SL., *Intradiscal pressure measurements above an instrumented fusion. A cadaveric study.* Spine, 1995. **20**: p. 526-531.
67. Rahm MD, H.B., *Adjacent-segment degeneration after lumbar fusion with instrumentation: A retrospective study.* Journal of Spinal Disorders & Techniques 1996. **9**: p. 342-400.
68. Whitecloud 3rd TS, D.J., Olive PM., *Operative treatment of the degenerated segment adjacent to a lumbar fusion.* Spine, 1994. **19**: p. 531-536.
69. Ghiselli G, W.J., Bhatia NN, Wellington KH, Dawson EG., *Adjacent segment degeneration in the lumbar spine.* The Journal of Bone and Joint Surgery 2004. **86**: p. 1497-503.
70. Bastian L., L.U., Thsch G, Blauth M., *Evaluation of the mobility of adjacent segment after posterior thoracolumbar fixation: A biomechanical study.* European Spine Journal 2001. **10**: p. 295-300.
71. Chou WY, H.C., Chang WN, Wong CY., *Adjacent segment degeneration after lumbar spinal posterior fusion with instrumentation in elderly patients.* Archives of Orthopaedic Trauma Surgery 2002. **122**: p. 39-43.
72. Lai P-L, C.L.-H., Niu C-C, Fu T-S, Chen W-J., *Relation between laminectomy and development of adjacent segment instability after lumbar fusion and pedicle fixation.* Spine, 2004. **29**: p. 2527-2532.
73. Chen CS, F.C., Cheng CK, Tzeng MJ, Liu CL, Chen WJ., *Biomechanical analysis of the adjacent to posterolateral fusion with laminectomy in lumbar spine.* Journal of Spinal Disorders & Techniques, 2005. **18**: p. 58-65.

74. Ahn Y-H, C.W.-M., Lee K-Y, Park K-W, Lee S-J., *Comparison of the load sharing characteristics between pedicle-based dynamic and rigid rod devices* Biomedical Materials 2008. **3**(4): p. 44101.
75. Meyers K, T.M., Sudin Y, Fleischer S, Arnin U, Girardi F, Wright T., *Use of instrumented pedicle screws to evaluate load sharing in posterior dynamic stabilization systems.* The Spine Journal 2008. **8**: p. 926-932.
76. V.K. Goel PhD, a.Y.E.K.P., *Effects of injury on the spinal motion segment mechanics in the axial compression mode* in *Department of Biomedical Engineering, College of Engineering*. 1989, University of Iowa: Lowa City.
77. Natarajan R.N., a.A.G.B.J., *Modeling the annular incision in a herniated lumbar intervertebral disc to study its effect on disc stability.* Computer Structures, 1997. **64**(5-6): p. 1291-1297.
78. Goel, V.K., Kong, W., Han, J.S., Weinstein, J.N., Gilbertson L.G., *A combined finite element and optimization investigation of lumbar spine mechanics with and without muscles. Spine*, 1993. **18**(11): p. 1531-1541.
79. Denoziere, G., *Numerical modeling of a ligamentous lumbar motion segment*, in *Mechanical Engineering*. 2004, Georgia Institute of Technology: Atlanta.
80. *Pitzen, T., Geisler, F.H,Matthis, D.,Storz, H.M., Pedersen, K.,and Steudel, W.I, The enfluence of cancellous bone density on load sharing in human lumbar spine: a comparison between an intact and a surgically altered motion segment.* Eur Spine, 2001. **10**: p. 23-29.
81. Tian-Xia MEng, Q., Teo Ee-Chon PhD., Lee Kim-Kheng Beng, Ng Hong-Wan MEng., Yang Kai MD., *Validation of T10-T11 Finite Element Model and Determination of Instantaneous Axes of Rotations in Three Anatomical Planes.* Biomechanics, 2003. **28**(24): p. 2694-2699.
82. L.J., G., *The mechanical behaviour of cancellous bone.* Biomechanica, 1985. **18**: p. 317-328.
83. Polikeit, A., *Finite element analysis of the lumbar spine: Clinical application*. 2002, University of Bern.
84. Shin, G., *Viscoelastic responses of the lumbar spine during prolonged stooping*, in *Ph.D. dissertation*. 2005, NCSU: USA.
85. Sairyo K., G.V.K., Masuda A.,Vishnubhotla S., et al., *Three-dimensional finite element analysis of the pediatric lumbar spine.* Eur Spine, 2006. **15**: p. 923-929.
86. Schultz A, W.D., Berkson M, Nachemson A, *Mechanical behavior of human lumbar spine motion segmenets - Part I. Responses in flexion, extension, lateral bending and torsion.* J Biomech Eng, 1979. **110**: p. 46-52.